Fundamental Research on Nonlinear Coupling between Nanomechanical Resonators exploiting Fano Resonance

Yang Bingda
Department of Applied Science and Technology
Politecnico di Torino

Supervisor

Prof. Stefano Stassi
Prof. Carlo Ricciardi

Acknowledgements

I wish to express my greatest gratitude to my supervisors Prof.Stefano Stassi and Prof.Carlo Ricciardi. They accepted me, a total amateur in their field, to finish my thesis in their lab. Especially, Prof. Stassi taught me knowledges and operations in the lab always with patience and professionalism. And to my girlfriend and the new pet, a German Shepherd, without whom this thesis would have been finished better and earlier.

Abstract

Micromechanical cantilevers are widely used in frequency-shift-based sensor of mass, force, and magnetic field. These devices are easily miniaturized with MEMS technology process and allow for integration with CMOS compatible electronics. Up to now, we don't have a fully detailed explanation of their dynamics response at their micro and nano scale, especially in the nonlinearity regime. Study of the dynamics response in micro and nano cantilevers grows rapidly, to satisfy the demands of fundamental questions and practical needs. Recently, direct observation of Fano resonances in coupled micro cantilevers arrays can greatly decrease the measuring time by parallelizing the measurements and the minimum detectable mass, thanks to an average ten-fold increase in Q factor of Fano peaks respect to Lorentzian ones. In this thesis, I demonstrate a method to study the shifts of Fano peaks induced by intermodal coupling. To implement this method, a signal generator is used to generate a group discrete excitation signals uprising slightly from a frequency below the resonance frequency to one up the resonance frequency. In the meanwhile, a lock-in amplifier is used to sweep and record an appropriate range of frequency in order to observe the shift of Fano resonance. A program of Labview is performed, in which a structure controls the signal generator giving the discrete uprising voltage while the lock-in amplifier sweeps and records. Shifts of Fano resonance become bigger as the

excitation signal increases because the changing stiffness of effective structure which can be induced by displacement. The shifts of Fano resonance are different when measuring between decreasing excitation signals and increasing excitation signals, which is similar to the Duffing phenomenon because of its bistability.

Contents

List of Figures

List of Tables

Chapter 1

Introduction

1.1 Atomic Force Microscopy

A cantilever is a rigid structural element, such as a beam or plate, fixed only at one end. Thanks to the discoveries of cantilevers with the dimension decreased to micro and nano scale level, these cantilevers are used in many fields. All these rapidly growing of discoveries results from the advent of AFM(atomic force microscopy) in 1986. With the help of this technology, characteristic of micro and nano cantilevers can be easily studied and become useful in realistic applications. Atomic force microscopy is a type of scanning probe microscopy with a resolution on the order of fractions of a nanometer, even more than 1000 times better than the optical diffraction limit. By the movement of piezoelectric elements, the surface information is gathered. The AFM consists of a cantilever with a sharp probe at its end that is used to scan surfaces. A piezoelectric element is placed at the other end to oscillate the cantilever at its eigenfrequency. A detector is used to detect the deflection and motion of the cantilever. The cantilever is typically with a tip radius curvature on the order of nanometers. When the tip is brought into a surface, forces between the tip and the surface cause a deflection of the cantilever according to Hooke's law. As the cantilever is displaced via its interaction with the surface, so too will the reflection of the laser beam be displaced on the surface of the photo diode. In order to interact with the surface, depending on the nature of the tip motion, the AFM can be operated at three modes.

1.1.1 Contact Mode

In this mode, the tip of the cantilever is swept across the surface of the sample with contact. And the contours of the surface are measured either using the deflection of the cantilever directly or, using the feedback signal from the cantilever that is kept from the sample at a constant distance. Close to the surface, attractive forces cause the tip of the cantilever to bend to the surface. Contact mode of AFM is usually done at a depth where the overall force is repulsive.

1.1.2 Tapping Mode

In most of the conditions, preventing the tip of the cantilever from sticking to the surface causing damage is a major problem to bypass. Nowadays, in tapping mode, the cantilever is driven to oscillate up and down at or near its resonance frequency. There is a small piezoelectric element in the cantilever holder to realize the oscillation. The frequency and amplitude of the driving signal are kept constant. If there is no drift or interaction with the surface, the cantilever oscillates at a constant amplitude. When the tip of the cantilever comes close to the surface of the sample, Van der Waals forces, dipole-dipole interactions, electrostatic forces cause the amplitude of the cantilever oscillation to decrease usually. The changed amplitude is used as the parameter to record the position of the tip of the cantilever to the surface.

1.1.3 Non-contact Mode

In this mode, the tip of the cantilever does not contact with the surface at all. The cantilever oscillates at its resonant frequency and the amplitude of the oscillation to the surface is typically a few nanometers down to a few picometers. The Van der Waals forces, which are the strongest from 1nm to 10nm above the surface, or any other long-range forces decrease the resonance frequency of the cantilever. By adjusting the average tip-to-sample distance, a constant oscillation amplitude of frequency is maintained. Measuring the tip-to-sample distance allows the AFM to construct a topographic image of the sample surface.

1.2 Micro and Nano cantilevers

A cantilever is a type beam which is supported and constrained at only one end. Based on this description, the Micro and Nano cantilevers are those decreased to micro and nano scale. In 1994, Itoh et al. fabricated a microcantilever coated with a thin layer of zinc-oxide with piezoelectric materials deposited. Then Cleveland et al. discovered the change of the resonance frequency when there is mass loading onto the microcantilever. Then Thundat et al. found bending of microcantilever can also be a method to detect mass on microcantilever.

Microcantilevers are used in a variety of micro electromechanical systems (MEMS) as micro transducers, sensors, switches, actuators, resonators, and probes. Particularly, the understanding of linear and nonlinear dynamic response of these micro-sized and nano-sized cantilevers is fundamental to many those applications. One of the methods to measure the bending of cantilever is monitored by focusing a laser beam at the tip of the cantilevers and recording the deflection of the reflected laser beam on a PSD(position sensitive detector). There are two detection mechanisms of microcantilever. The first operating mechanism of cantilever is the so-called static mode. Cantilevers deformation can be induced by thermal expansions, surface stress changes and so on.

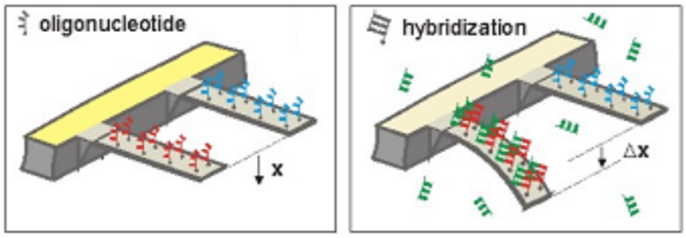

Figure 1.1: Bending of the cantilever due to the generated surface stress by absorption with stimuli in static mode [1]

Based on the features of static mode, for example thermal expansions, temperature can be measured by a cantilever made by two layers of different materials is sensible to temperature variations. The different thermal expansions of the two layers cause a thermally induced stress and the cantilever will bend statically. With careful calculations and calibrations, the temperature can be read out by bending of a cantilever. That is called a temperature sensor.

Independently of thermal effects, molecular adsorption processes and facial chemical reactions can cause a change in mechanical stress. A beam deflection can also be revealed and associated with the beam interaction with external stimuli, physical, mechanical, chemical, biological and so on. In this case, cantilevers deformation is related to a gradient of mass absorption those external stimuli. Despite the physical adsorption, inter facial chemical reactions may also affect mechanical stresses in thin plates more directly. To serve as a sensor to detect these stimuli, cantilevers can be coated with a sensing layer, whether this layer can absorb molecular of the stimuli physically causing bending of the cantilever by generating the surface stress or react with stimuli chemically. By coating such layers with particular materials, the cantilever can be made into sensors to detect different materials in gas or liquid.

Another operating mechanism of cantilever is dynamic operation mode. In this mode, the cantilevers keep vibrating in gas, in vacuum or in liquid. That can be treated as damped mechanical oscillators.The motions of cantilever is affected by the mass of cantilevers. A mass variation can be reflected on a changing resonance frequency. By this resonance frequency shift-based approach, the amount of mass adsorbed by the cantilever can be evaluated. Furthermore, the quantity of chemical stimuli or biological stimulus can also be evaluated if one mass of sample is measured.

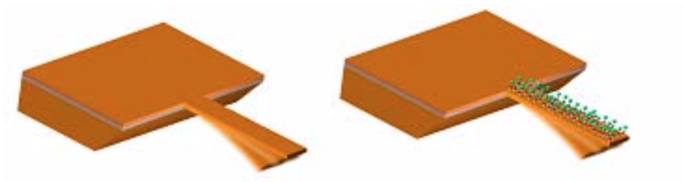

Figure 1.2: Dynamic mode of a microcantilever [1]

1.3 Fano resonance phenomenon

Ugo Fano, an Italian-American physicist, first gave a theoretical explanation for the asymmetric shape that is due to a interference of a continuum state and an excitation of discrete state. The frequency of the resonant state must lie in the frequency range of the continuum states for the effect to occur. Near the resonant frequency, the background amplitude typically varies slowly with frequency while the resonant amplitude changes both in magnitude and phase quickly. This non symmetric variation creates the asymmetric shape.

Fano used a perturbation approach explain the appearance of asymmetric resonances. As a result he obtained the formula for the shape of the resonance shape.

$$\sigma = \frac{(\epsilon + q)^2}{\epsilon^2 + 1} \tag{1.1}$$

Shape parameter q and reduced energy ϵ are defined by $2(E - E_F)/\tau$, where E_F is resonance energy, when the discrete state energy is equal to the continuum state energy, $E_f = 0$, that is E_0, and τ is the width of the auto-ionized state. This equation suggests that there are exactly maximum and minimum of results, that is the maximum and minimum of the amplitude of the Fano resonance.

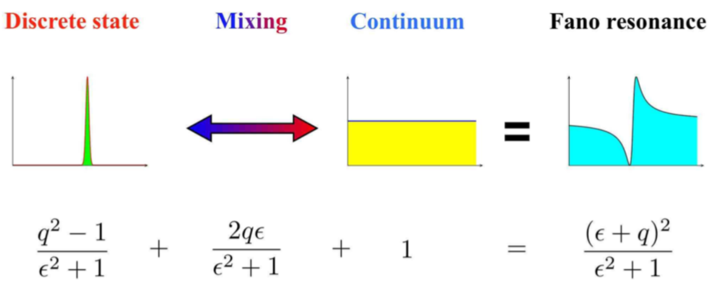

Figure 1.3: Fano resonance is consist of a continuum state and an excitation state [2]

$$\sigma_{min} = 0, \quad at \quad \epsilon = -q\sigma_{max} = 1 + q^2, \quad at \quad \epsilon = \frac{1}{q} \tag{1.2}$$

Considering this parameter q, a ratio of transition probabilities to the mixed state and to the continuum. For different q, the shapes are different.

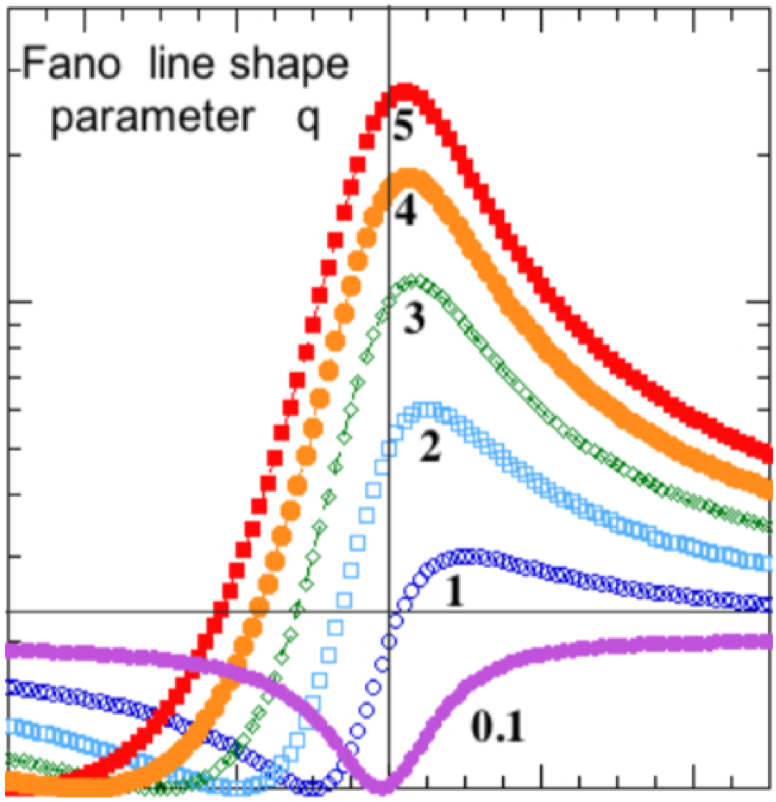

Figure 1.4: For different q, the shapes of Fano resonance are different

Examples of Fano resonances can be found in atomic physics, nuclear physics, condensed matter physics, circuits, microwave engineering, nonlinear optics, photoelectronic, magnetic meta materials, and in mechanical waves. Thanks to the first experimental evidence of Fano resonance purely in coupled micro and nano mechanical cantilever arrays. [3]In our measurement, Fano resonance is used as a tool or a symbol to study the non linearity in coupled micro and nano cantilevers. Because all the resonance frequency of all cantilevers of a microcantilever array can be found by measuring resonance frequency of only one cantilever and Fano resonance of its corresponding coupled cantilevers.

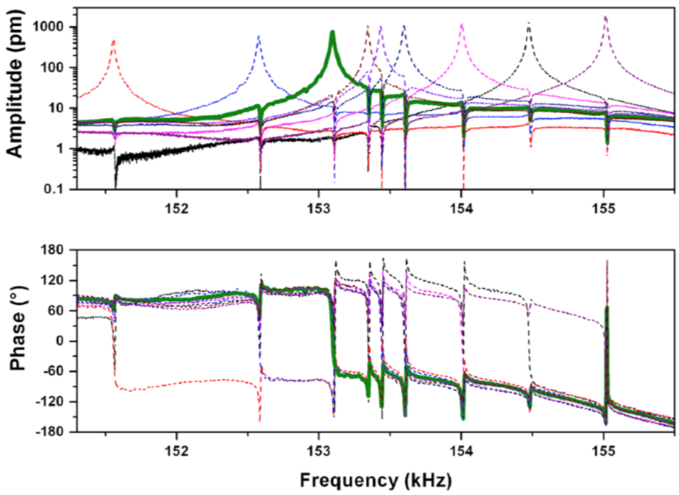

Figure 1.5: Fano resonance in a microcantilever array [3]

Chapter 2

Theory

2.1 Vibration of Cantilevers

Cantilevers are suspended structures, fixed at one, while the other end is free to bend in Figure 2.1.

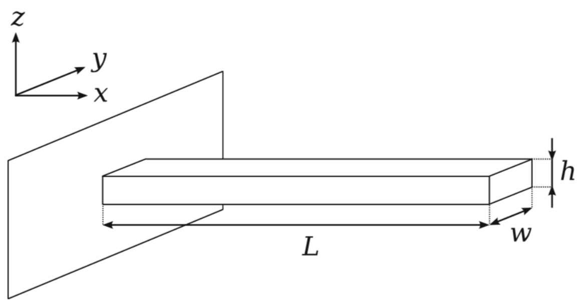

Figure 2.1: A schematic of a cantilever, where L, w, h represent the length, width, and height [4]

This, the most common Micromechanical and nano mechanical structure, can be modeled by Euler-Bernoulli beam theory. To study the bending behavior of this structure, assuming that all beams are thin and long are applied, at least lengths is 10 times greater than heights. According to Euler-Bernoulli beam theory, assuming a linear elastic material and small deflection $u_{(x,t)}$ the equation of motion of a thin beam is given by

$$\rho A \frac{\partial^2 u(x,t)}{\partial t^2} + EI_Y \frac{\partial^4 u(x,t)}{\partial x^4} = 0 \tag{2.1}$$

Where ρ is the mass density, A is the cross sectional area, E is the Young's modulus and I_Y is the geometric moment of inertia. The solution to this differential equation can be separated into a position dependent and a time-dependent term via a separation of variables.

$$u(x,t) = \sum_{\infty}^{n=1} U_n(x) \cos(\omega t) \tag{2.2}$$

Where ω is the frequency of motion and n denotes the modal number. A general solutions to the displacement function of the beam $U_n(x)$ can be described as

$$U_n(x) = a_n \cos \beta_n x + b_n \sin \beta_n x + c_n \cosh \beta_n x + d_n \sinh \beta_n x \tag{2.3}$$

Where β_n is the wavenumber. The first two terms represent the standing waves in the beam center, while the last two represent the influence of the clamping.

For a particular beam, the boundary conditions of a cantilever are described by

$$U_n(0) = \frac{\partial}{\partial x} U_n(0) = \frac{\partial^2}{\partial x^2} U_n(L) = \frac{\partial^3}{\partial x^3} U_n(L) = 0 \tag{2.4}$$

A system of linear equations of fourth order can be written as

$$\begin{bmatrix} 1 & 0 & 1 & 0 \\ 0 & 1 & 0 & 1 \\ -\cos(\beta_n L) & -\sin(\beta_n L) & \cosh(\beta_n L) & \sinh(\beta_n L) \\ \sin(\beta_n L) & -\cos(\beta_n L) & \sinh \beta_n L & \cosh(\beta_n L) \end{bmatrix} \begin{pmatrix} a \\ b \\ c \\ d \end{pmatrix} = \begin{pmatrix} 0 \\ 0 \\ 0 \\ 0 \end{pmatrix} \tag{2.5}$$

A non-trivial solution exists for this homogeneous system if the determinant is zero, that is

$$\cos(\beta_n L)\cosh(\beta_n L) + 1 = 0 \tag{2.6}$$

Obviously, this equation has discrete solutions for specific wavenumber, which are related to eigenfrequency of the cantilever. This equation can be solved numerically for the lower order modes. Considering higher eigenvalues, this equation can be simplified to

$$\cos(\beta_n L) \approx 0 \qquad \forall n \geq 3 \tag{2.7}$$

and

$$\beta_n L \approx (2n-1)\pi/2 \tag{2.8}$$

In conclusion, the roots of this frequency equation of a cantilever beam are

$$\lambda_n = \beta_n L = 1.8751, 4.6941, 7.8548, (2n-1)\pi/2 \tag{2.9}$$

And the eigenfrequency of a cantilever can write as

$$\Omega_n = \frac{\lambda_n^2}{L^2}\sqrt{\frac{EI_y}{\rho A}} \tag{2.10}$$

Considering the first two boundary conditions of the mode shape function $U_n(x)$, with the third boundary condition we obtain the ratio of the coefficients $a_n \quad and \quad b_n$

$$\frac{\partial^2}{\partial x^2}U_n(L) = 0 : \frac{b_n}{a_n} = -\frac{\cos(\beta_n L) + \cosh(\beta_n L)}{\sin(\beta_n L) + \sinh(\beta_n L)} \tag{2.11}$$

A general solutions to the displacement function of the beam can be written in the form

$$U_n(x) = a_n[\cos\beta_n x - \cosh\beta_n x - \frac{\cos(\beta_n L) + \cosh(\beta_n L)}{\sin\beta_n L + \sinh(\beta_n L)}](\sin\beta_n x - \sinh\beta_n x) \tag{2.12}$$

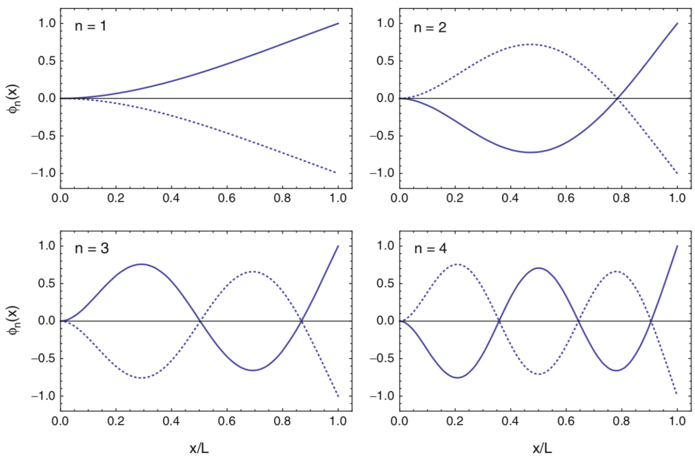

Figure 2.2: Four vibration modes of a cantilever [4]

First four modes of a cantilever are shown in Figure2.2. In particular mode, some parts of the cantilever move to the longest distance comparing to static mode, while some node remain static. The number of static nodes increases along with numbers of modes.

2.2 Coupling among Oscillators

2.2.1 Damped Linear Resonator

A lumped model simplifies the description of the behavior of spatially distributed physical systems into a topology consisting of discrete entities that approximate the behavior of the distributed system under certain assumptions. It is useful in electrical systems (including electronics), mechanical multi body systems, heat transfer, acoustics, etc. Mathematically speaking, the simplification reduces the state space of the system to a finite dimension, and the partial differential equations (PDEs) of the continuous (infinite-dimensional) time and space model of the physical system into ordinary differential equations (ODEs) with a finite number of parameters. Vibration energy can transfer from kinetic to elastic elements such as beams, strings and plates. These structures store potential energy in terms of deformation energy. A general lumped model, consist of a spring, a mass, a force and a damping factor in Figure 2.3 describes this periodic conversion of such energy transfer. The mechanical behavior of this modal is generally approximated by a linear relation between the continuum stressσ and strainε

$$\sigma = E\varepsilon \tag{2.13}$$

where E is the Young's modulus.

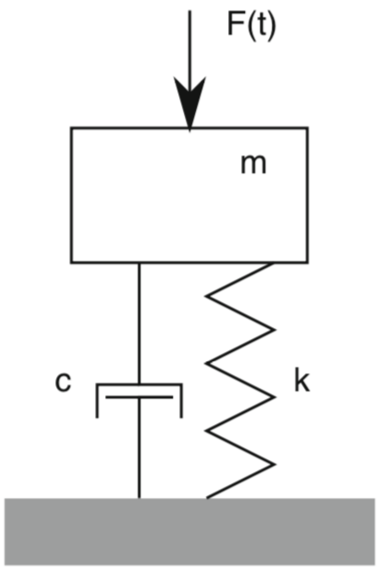

Figure 2.3: A lumped mass-spring model [4]

When a resonator is driven in the linear regime, the dynamics can be simplified by a one-dimensional resonator oscillator based on a linear zero mass spring. Assuming a periodic driving force

$$F(t) = F_0 \cos(\omega t) \tag{2.14}$$

A second order differential equation of this model, a linear damping element, a mass and a linear zero mass spring, is

$$m\ddot{z} + c\dot{z} + kz = F(t) \tag{2.15}$$

Where m is the total mass, k is the spring constant, and c is the coefficient of damping force.

Free Undamped Vibration

With none damping, the total energy of the system remains constant. During oscillation the total energy is fully giving and returned between kinetic and potential energy. The system turns totally into an oscillator with no driven force. According to the method used to obtain this good approximation which is called $Rayleigh's\ method$, the maximal kinetic energy must be equal to the maximal potential energy. That is

$$m\ddot{z}^2 = kz^2 \tag{2.16}$$

From this equation, the eigenfrequency Ω of the undamped free mechanical system can be denoted

$$\Omega = \omega = \sqrt{\frac{k}{m}} \tag{2.17}$$

Free damped Vibration

Unavoidably, there is damping factor in realistic environment. Without a driven force, the equation of the lumped linear model reduces to

$$\ddot{z} + 2n_c\dot{z} + \Omega z = 0 \tag{2.18}$$

where the coefficient of damping n_c is defined

$$n_c = \frac{c}{2m} \tag{2.19}$$

Another parameter damping ratio is defined by

$$\zeta = \frac{n_c}{\Omega} \tag{2.20}$$

By applying Euler's formula, and setting $z = z_0 e^{\gamma t}$, the equation to describe the free damped vibration can be rewrite as

$$z(t) = z_0 e^{-\Omega\zeta t} \cos(\Omega\sqrt{1-\zeta^2 t}) \tag{2.21}$$

Through the above equation, the free damped vibration has an exponentially decaying oscillation with a frequency $\omega_{nature} = \Omega\sqrt{1-\zeta^2}$, this frequency is called natural frequency.

Driven damped Vibration

The most common way to actuate a mechanical cantilever is by shaking its base by a piezoelectric element. To denote the equation of this vibration, first insert $z(t) = z_0 e^{i\omega t}$ into the original free damped vibration equation as a specific steady solution. This specific solution takes the form

$$z(t) = \frac{F_0/m}{\sqrt{(\Omega^2 - \omega^2)^2 + 4\zeta^2\Omega^2\omega^2}} \cos(\omega t + \varphi) \tag{2.22}$$

Both the amplitude and phase response as a function of the relative frequency ω/Ω can be denoted from the above equation. The amplitude is

$$|z_0| = \frac{F_0/k}{\sqrt{(1 - (\frac{\omega}{\Omega})^2)^2 + 4\zeta^2(\frac{\omega}{\Omega})^2}} \tag{2.23}$$

While the phase is

$$\arg(z_0) = \varphi = \arctan\frac{2\zeta(\frac{\omega}{\Omega})}{(\frac{\omega}{\Omega})^2 - 1} \tag{2.24}$$

where F_0/k represents the static deflection, then the dynamic amplification is simply given by

$$\delta z_0 = \frac{1}{\sqrt{(1 - (\frac{\omega}{\Omega})^2)^2 + 4\zeta^2(\frac{\omega}{\Omega})^2}} \tag{2.25}$$

In the case just mentioned above, the relative amplitude and phase of the vibration actuated by a piezoelectric element can be described by

$$\delta z_0 = \frac{(\frac{\omega}{\Omega})^2}{\sqrt{(1 - (\frac{\omega}{\Omega})^2)^2 + 4\zeta^2(\frac{\omega}{\Omega})^2}} \tag{2.26}$$

and the phase

$$\arg(z_0) = \varphi = \arctan\frac{2\zeta(\frac{\omega}{\Omega})}{1 - (\frac{\omega}{\Omega})^2} \tag{2.27}$$

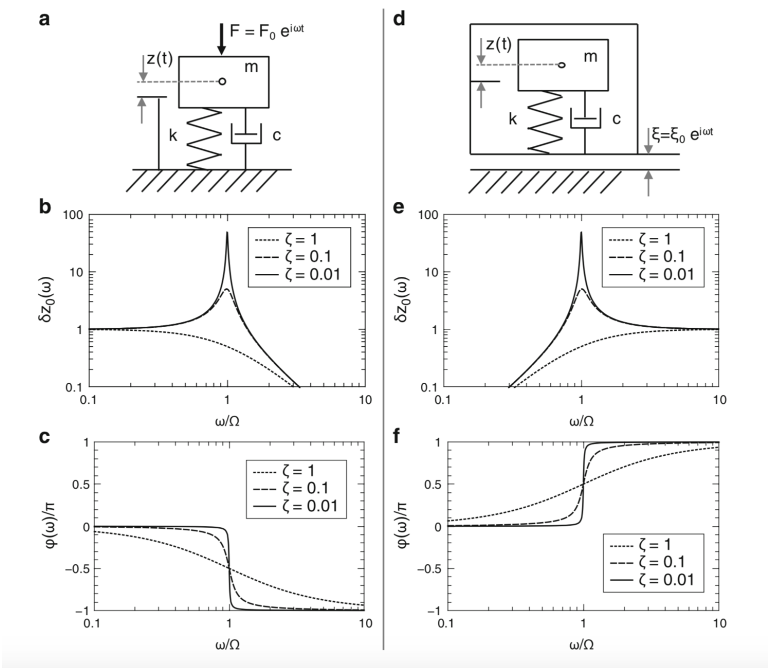

Figure 2.4: A lumped model of driven damped vibration. (a) driven by a force and (b) driven by an external vibration (b) and (e) show the relative amplitude response, (c) and (f) show the respective phase responses [4]

Driven damped vibration system is shown in the Figure 2.4 with two conditions, driven by a force and by another vibration.

2.2.2 Quality Factor

In physics, quality factor is a dimensionless parameter that describes how sharp the peak of the resonance. This parameter characterizes a resonator's bandwidth relative to its resonance frequency. High Q factor indicates a lower rate of energy loss relative to the stored energy of the resonator, the oscillations die out more slowly. The physical definition is the ratio between the energy stored and energy lost during one cycle at resonance

$$Q = 2\pi \frac{W}{\Delta W} \tag{2.28}$$

Where W is the total energy stored in the system and δW is the energy loss during one cycle of oscillation. Instead of fitting with the oscillator model, the measured resonance curves are fitted with a *Lorentzian* function. The extraction of Q is then based on the $-3dB$ *bandwidth method. The* $-$ $3dB$ *bandwidth method* is based on the definition of Q in electrical resonant circuit where quality factor is given by

$$Q = \frac{\omega_r}{\Delta\omega_{-3dB}} = \frac{1 - 2\zeta^2}{2\zeta} \tag{2.29}$$

Where $\Delta\omega_{-3dB}$ is the frequency difference between the two frequencies at which the amplitude curve has the half maximum energy $B\sqrt{2}(-3dB)$. For small damping, this definition of the quality factor is equal to the physical one. The quality factor can now be found by measuring the amplitude response around the resonance. The resonance frequency divided by the $-3dB$ bandwidth is an approximation for Q small damping.

2.2.3 Linear Coupling

Strong Coupling

Particularly, ultra sensitive mass detection and identification can be realized by arrays of coupled micro and nano cantilevers. Usually Lorentzian peaks are used in single cantilever and strongly coupled micro and nano cantilever arrays.Besides this, more and more various applications from dynamics of coupled micro and nano cantilever arrays draw greater and greater attentions. Let's consider a real world coupled Micromechanical resonator pair.

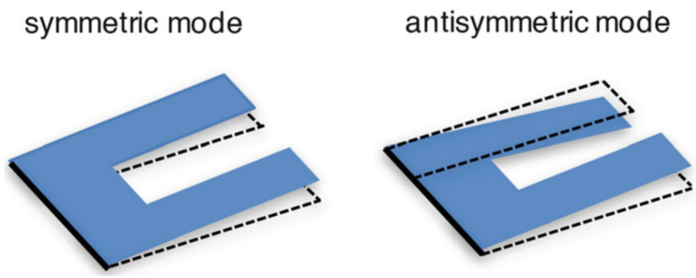

Figure 2.5: Two linear coupled cantilevers [4]

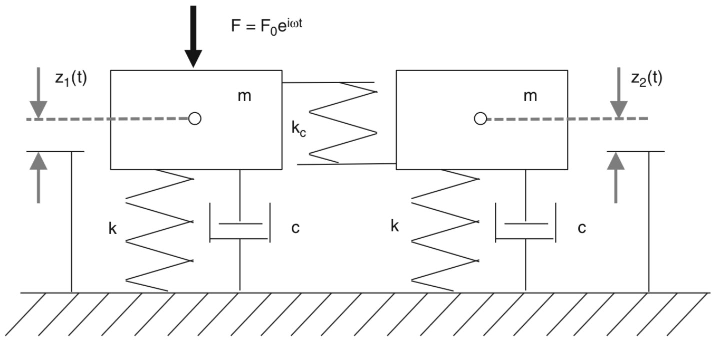

Figure 2.6: A lumped model of two linear coupled cantilevers [4]

Two cantilevers are coupled via a shared overhang between the structures. To calculate the eigenfrequency of the coupled resonators, the homogenous undamped system is described here.

Considering Newton's second law yields the equation of motion

$$m\ddot{z}_1 + kz_1 + k_c(z_1 - z_2) = 0 \qquad m\ddot{z}_2 + kz_2 - k_c(z_1 - z_2) = 0 \tag{2.30}$$

Plugging in the standard ersatz, which yields the Ω_s linear system of equation

$$\begin{pmatrix} -\omega^2 m + k + k_c & -k_c \\ -k_c & -\omega^2 m + k + k_c \end{pmatrix} \begin{pmatrix} A_1 \\ A_2 \end{pmatrix} = \begin{pmatrix} 0 \\ 0 \end{pmatrix} \tag{2.31}$$

Setting the determinant of the system is zero, we can find the non-trivial solutions

$$(-\omega^2 + k + k_c)^2 - k_c^2 = 0 \tag{2.32}$$

which yields two positive eigenfrequency

$$\omega_1 = \Omega_s = \sqrt{\frac{k}{m}} \qquad \omega_2 = \Omega_a = \sqrt{\frac{k + 2k_c}{m}} \tag{2.33}$$

Giving $A_1 = A_2 \quad for \quad \Omega_s \qquad A_1 = -A_2 \quad for \quad \Omega_a$ For symmetric mode at the eigenfrequency $\Omega_s$both vibrational amplitudes of resonators are equal. The normal mode eigenfrequency is equal to the one of a single uncoupled resonator. Since both resonators are vibrating in the same phase, there is no displacement-induced tension between resonators. When vibrating at the other eigenfrequency Ω_a the two vibrating resonators are moving in opposite direction and the coupling spring causes displacement-induced tension, which increases the normal mode eigenfrequency. Also, the response of a damped and driven system can be calculated from the corresponding system of equations

$$m\ddot{z}_1 + c\dot{z}_1 + kz_1 + k_c(z_1 - z_2) = F_0 e^{i\omega t} \qquad m\ddot{z}_2 + c\dot{z}_2 + kz_2 - k_c(z_1 - z_2) = 0 \tag{2.34}$$

Weakly Coupling(Fano Resonance)

In our case, Fano resonance is found in weakly coupled cantilever arrays with a dimension like micro or nano scale. A theoretical model based on weak elastic and damped coupling is described. In our experimental set-up, the whole array is sticked to the piezoactuator in a vacuum chamber. All the cantilevers in the array are subjected to the same external excitation force. Each cantilever n (with n=1,2) is modeled by a damped harmonic oscillator consisting of active mass m_n, structure dissipation c_n and bending stiffness k_n. However, in this description, we only consider $n = 1, 2$. A weak coupling spring factor k_{12} is used so that the two eigenfrequency modes were negligibly replaced from solutions of independent oscillators and with a damping factor c_{12}.

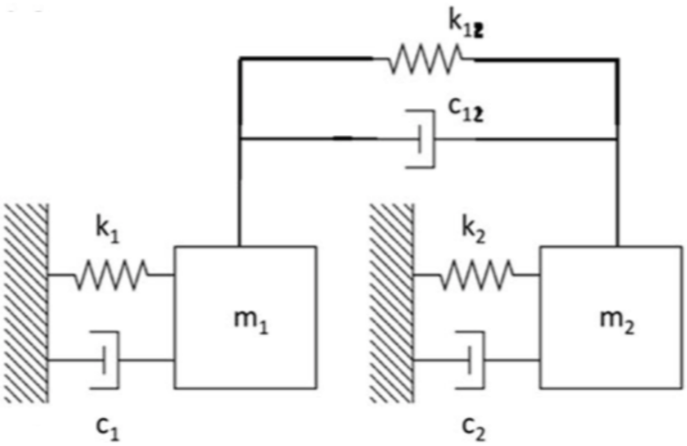

Figure 2.7: A lumped model of two weakly coupled cantilevers [3]

An external periodic driving force $F \cdot e^{i\omega t}$ is applied to the following equations.

$$\ddot{x_1} + \gamma_1 \dot{x_1} + \omega_1^2 x_1 + \upsilon_{12}(x_1 - x_2) + \gamma_{12}(\dot{x_1} - \dot{x_2}) = F \cdot e^{i\omega t} \tag{2.35}$$

$$\ddot{x_2} + \gamma_2 \dot{x_2} + \omega_2^2 x_2 + \upsilon_{21}(x_2 - x_1) + \gamma_{21}(\dot{x_2} - \dot{x_1}) = F \cdot e^{i\omega t} \tag{2.36}$$

where $\omega_n = \sqrt{k_n/m_n}$ are the natural frequency of the single resonators, $\gamma_n = c_n/m_n$ are the frictional parameter and $\upsilon_{12} = \upsilon_{21} = k_{12}/m_n$ and $\gamma_{12} = \gamma_{21} = c_{12}/m_n$ are the elastic and damping coupling between the cantilevers. The forced response of a damped system has the same frequency as the excitation force, but with different amplitudes and phases, the solutions of the system can be assumed as

$$x_{1,2} = X_{1,2}(\omega) e^{i\omega t} \tag{2.37}$$

then the complex amplitude can be written as

$$a_1(\omega) = \frac{(\omega_2^2 - \omega^2 + i\gamma_2\omega + 2\upsilon_{12} + 2i\gamma_{12}\omega)}{(\omega_1^2 - \omega^2 + i\gamma_1\omega)(\omega_2^2 - \omega^2 + i\gamma_2\omega) + \upsilon_{12}(\omega_1^2 - \omega^2 + i\gamma_1\omega) + \upsilon_{12}(\omega_2^2 - \omega^2 + i\gamma_2\omega) + i\gamma_{12}\omega(\omega_1^2 - \omega^2 + i\gamma_1\omega) + i\gamma_{12}\omega(\omega_2^2 - \omega^2 + i\gamma_2\omega)} F \tag{2.38}$$

$$a_2(\omega) = \frac{(\omega_1^2 - \omega^2 + i\gamma_1\omega + 2\upsilon_{12} + 2i\gamma_{12}\omega)}{(\omega_1^2 - \omega^2 + i\gamma_1\omega)(\omega_2^2 - \omega^2 + i\gamma_2\omega) + \upsilon_{12}(\omega_1^2 - \omega^2 + i\gamma_1\omega) + \upsilon_{12}(\omega_2^2 - \omega^2 + i\gamma_2\omega) + i\gamma_{12}\omega(\omega_1^2 - \omega^2 + i\gamma_1\omega) + i\gamma_{12}\omega(\omega_2^2 - \omega^2 + i\gamma_2\omega)} F \tag{2.39}$$

The definition of the real amplitude of the cantilever is the modulus as following,

$$a_n(\omega) = |a_n(\omega)|\, e^{i\varphi_n(\omega)} \tag{2.40}$$

This numerical solutions for the two weakly coupled cantilevers obtained from the equations are in good agreement with the experimental curves of a vibrating array.

2.2.4 Non Linear Coupling

Non linear coupling oscillator can be separated into two types. In order to understand the two types of non linear coupling, we can simply solve the equations which describes the motions.

Duffing oscillator

Duffing oscillator is one kind of damped and driven oscillators, whose dynamics can be described by a non-linear second-order differential equation

$$\ddot{x} + \delta\dot{x} + \alpha x + \beta x^3 = \gamma\cos(\omega t) \tag{2.41}$$

Where δ controls the amount of damping, α controls the linear stiffness, β controls the amount of nonlinear in the restoring force; if $\beta = 0$, the Duffing equation describes a damped and driven simple harmonic oscillator; For a linear oscillator with $\beta = 0$, the frequency response is also linear. γ is the amplitude of the periodic driving force; if $\gamma = 0$, the system is without a driving force and ω is the angular frequency of the periodic driving force. z is the amplitude of response. This equation describes the motion of a damped oscillator with a more complex potential than in simple harmonic motion. In physical terms, this equation models a spring pendulum whose spring's stiffness does not exactly obey Hooke' law. In another word, the duffing equation describes the oscillations of a mass attached to a nonlinear spring and a linear damper. The restoring force of the nonlinear spring is $\alpha x + \beta x^3$. When $\alpha > 0$ *and* $\beta > 0$, the spring is called a hardening spring. Conversely, for $\beta < 0$, it is a softening spring. In a word, for a non zero cubic coefficient, the frequency response becomes nonlinear. With different parameters, the Duffing oscillator can show hardening , softening or mixed hardening-softening frequency response.

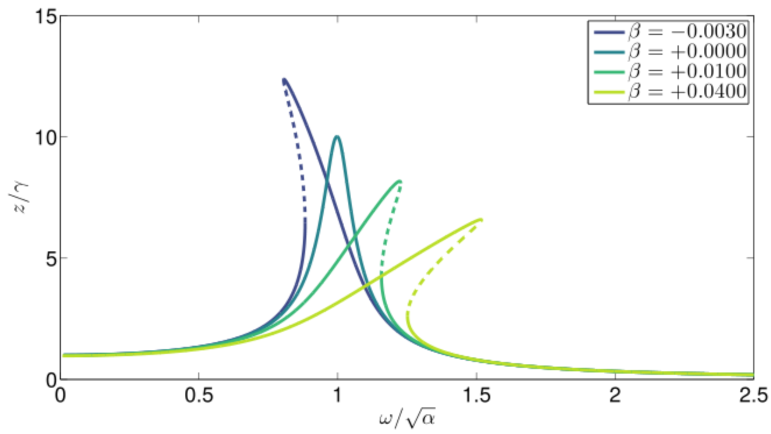

Figure 2.8: Frequency response of duffing equation with different β [5]

For certain ranges of the parameters in the duffing equation, the frequency response may no longer be a single-valued function of forcing frequency ω . For a hardening spring oscillator, the frequency response overhangs to the high-frequency side, and to the low-frequency side for the softening spring oscillator. When the angular frequency ω is slowly increased(with other parameter fixed), the response amplitude z drops at A suddenly to B. Conversely, if the angular frequency ω is slowly decreased, then at C the amplitude jumps up to D, thereafter following the upper branch of the frequency response.

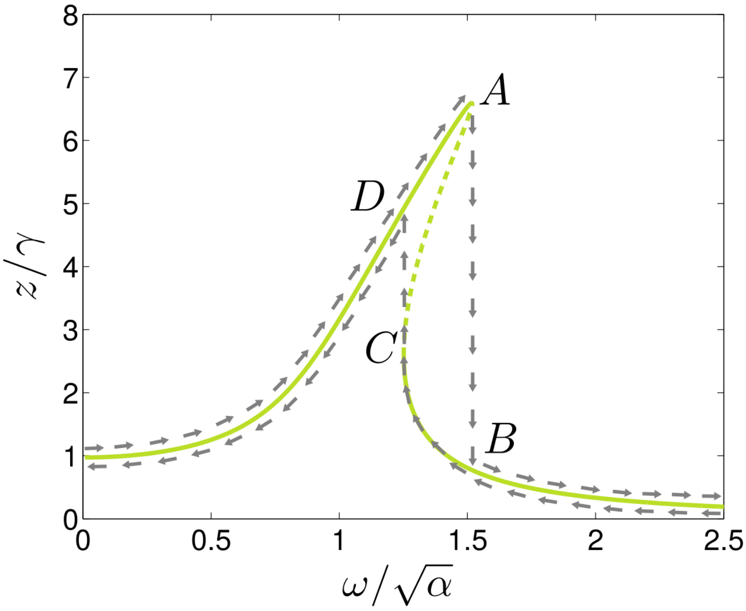

Figure 2.9: Jumps phenomenon [6]

The jumps A-B and C-D do not coincide, so the system shows hysteresis depending on the frequency sweep direction.

Van der Pol oscillator

Van der Pol oscillator is non-conservative oscillator with nonlinear damping, in which energy in added to and subtracted from the system in an autonomous method, resulting in a periodic motion called a limit cycle. A second-order differential equation describes its dynamics.

$$\frac{\mathrm{d}^2x}{\mathrm{d}t^2} - \mu(1-x^2)\frac{\mathrm{d}x}{\mathrm{d}t} + x = 0 \tag{2.42}$$

Where x is the position coordinate-which is a function of the time t, and μ is a scalar parameter indicating the nonlinearity and the strength of the damping. For the unforced Van der Pol Oscillator, when $\mu = 0$, there is no damping function, the equation becomes

$$\frac{\mathrm{d}^2x}{\mathrm{d}t^2} + x = 0 \tag{2.43}$$

This is a form of the simple harmonic oscillator and there is always conservation of energy. When $\mu < 0$, the system becomes a simple vibration with damping. When $\mu > 0$, the system will enter a limit cycle. Near the origin $x = \mathrm{d}x/\mathrm{d}t = 0$, the system is unstable and far from the origin, the system is damped.

For forced Van der Pol Oscillator, when a forced sinusoidal driving signal $A\sin(\omega t)$ is added to the unforced system, the equation to describe the system becomes

$$\frac{\mathrm{d}^2x}{\mathrm{d}t^2} - \mu(1-x^2)\frac{\mathrm{d}x}{\mathrm{d}t} + x - A\sin(\omega t) = 0 \tag{2.44}$$

Where A is the amplitude, or displacement, of the wave function and ω is its angular velocity. The forced Van der Pol Oscillator shows deterministic chaotic behavior.

2.2.5 Intermodal Coupling Nonlinearity

When only one of the vibrational modes is driven, a micro and nano mechanical resonator is modeled as a SDOF(single degree of freedom) oscillator. When two or more of these vibrational modes are excited, the single resonator system should be modeled as MDOF(multi degree of freedom) oscillators coupled with each other while the engaged modes are coupling among each others, this is called intermodal coupling.

For now, there hasn't a complete theoretical model to describe the dynamic

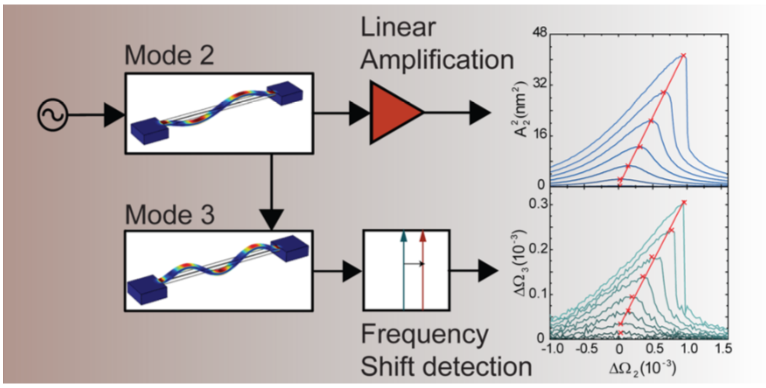

Figure 2.10: General description of the creation of Matheny et al [7]

of intermodal coupling. But many scientists published some paper to study this dynamic.

Matheny et al(2013), created an experimental protocol to study the device nonlinearities, especially NEMS. In their work, a doubly clamped beam was used for the intra and intermodal nonlinearities, compared with predictions from Euler-Bernoulli theory [7].

Measures using the procedure described in this article and calculations from Euler-Bernoulli theory are in good agreement. They used intermodal coefficients to predict the dynamics.

By the work of Atakan et al(2018), intermodal coupling was used as a probe for detecting nano mechanical modes. To implement this method, they used a probe mode as a excitation voltage and monitored by a phase-locked-loop, while another auxiliary excitation signal scanned for other modes. When the auxiliary excitation signal exciting the corresponding mode around its resonance frequency, the displacement-induce tension caused a frequency shift in the probe mode. They also used the location and width of these frequency shifts to determine the frequency and quality factor of mechanical modes. Their work is quite indicating for our measure [8].

Coupling between modes happens due to the increased tension along the beam

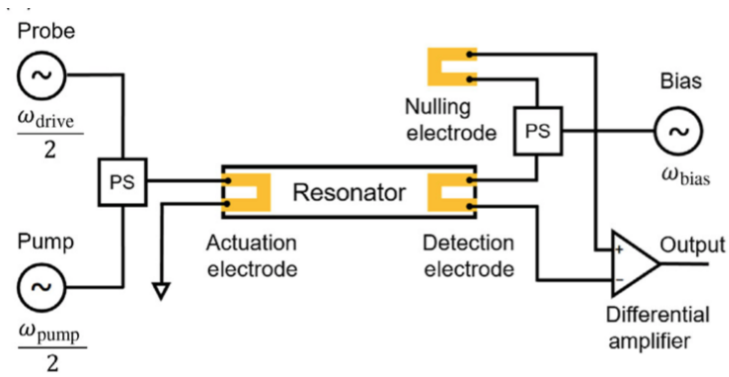

Figure 2.11: Block diagram of Atakan et al's work, actuation and readout scheme to pump and detect higher-order modes while simultaneously tracking a specific resonance mode with PLL [8]

axis which changes the effective stiffness of the mechanical structure. In their experiments, the frequency shift in the measured probe mode k due to the excitation of a pump mode j can be calculated as

$$\Delta\omega = \omega_k - \omega_{k,initial} = \omega_{k,initial} g_{kj} a_j^2 \tag{2.45}$$

where g_{kj} is the coupling coefficient between modes j and k. As the oscillation amplitude of mode a_j starts from zero and increases, the frequency shift they observed in the probe mode k can be related to the amplitude of the pump mode j. In this way, they can indicate the location of the pump mode frequency by the location of the frequency shift. Further more, the magnitude of the frequency shift is used to indicate the square of amplitude. [8]

Our measurement is also to find fundamental behaviors of intermodal coupling resonators. Nonlinear intermodal coupling can be easily triggered via displacement-induce tension in the structure of beams, tubes and membranes. This nonlinear intermodal coupling is similar to the hardening behaviors modeled by a Duffing equation for a SDOF system. In this regime, the dynamic of the nonlinear is not fully studied and more fundamental research is needed.

Chapter 3

Experimental Preparation

3.1 Fabrication

In our case, the Microcantilevers are fabricated from SOI substrate in Chilab laboratory of the Polytechnic of Turin, which is located in Chivasso. The fabrication is done by the following steps:

- SOI substrates replace conventional silicon substrate in semiconductor manufacturing. The SOI technology refers to the use of a layered silicon insulator silicon substrate in place of conventional silicon substrates in semiconductor manufacturing, especially microelectronics, to reduce parasitic device capacitance, thereby improving performance. These substrates are widely used, in particular into fabricating cantilevers, membranes and bridges.
- A polymeric protective coating is deposited on top of the SOI substrates. On the back of SOI substrates, a photoresist is deposited where are and the part to be removed exposed with UV light.
- By photolitographic step and BOE solution etching, the silicon oxide is cleared away. The BOE(Buffered oxide etch) solution is a mixture of

a buffering agent, such as ammonium fluoride(NH_4F) and hydrofluoric acid(HF).

- Then a KOH(Potassium hydroxide) solution is used to remove the silicon bulk, creating cantilever area.

- Another photolitographic step is performed after cleaning the sample. The part that are not covered by the photoresist is etched through RIE(Reactive-ion etching) etching. This frees one side of the cantilever.

- With carefully calculation, BOE solution remove the sacrificial layer of silicon dioxide.

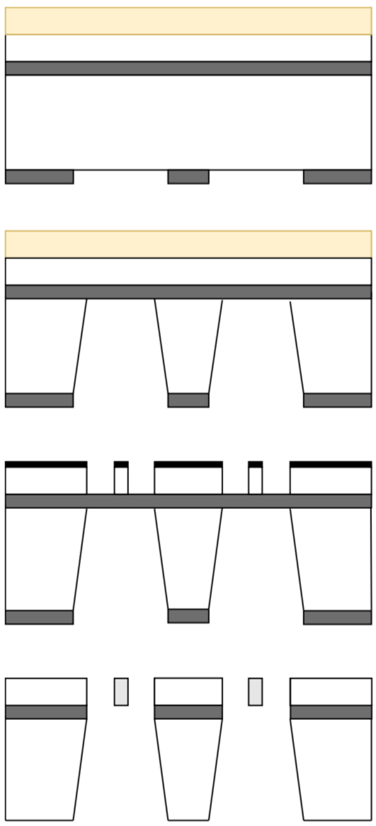

Figure 3.1: Fabrication process of a microcantilever array

3.2 Instrument Set-up

In our measurement, the commercial machine used is called MSA-500 micro system analyzer from a company Polytec. The MSA-500 micro system analyzer was designed to combine several measurement techniques into a convenient "All-in-One" solution for characterizing surface metrology and measuring in-plane and out-of-plane motions. This instrument delivers increased measurement flexibility and precision, adapting to the needs of today's and tomorrow's micro structures. When incorporated in the MEMS design and test cycle, the Micro System Analyzer provides precise 3-D dynamic and static response data that increases device performance while reducing development and manufacturing costs through enhanced and shortened design cycles, simplified trouble shooting and improved yield.

Figure 3.2: A commercial system called MAS-500

The laser-Doppler vibrometer is a precision optical transducer for determining the vibration velocity and displacement at a measurement position. It works by sensing the frequency shift of back scattered light from a moving surface. The object scatters or reflects light from the laser beam and the Doppler frequency shift is used to measure the component of velocity which lies along the axis of the laser beam.

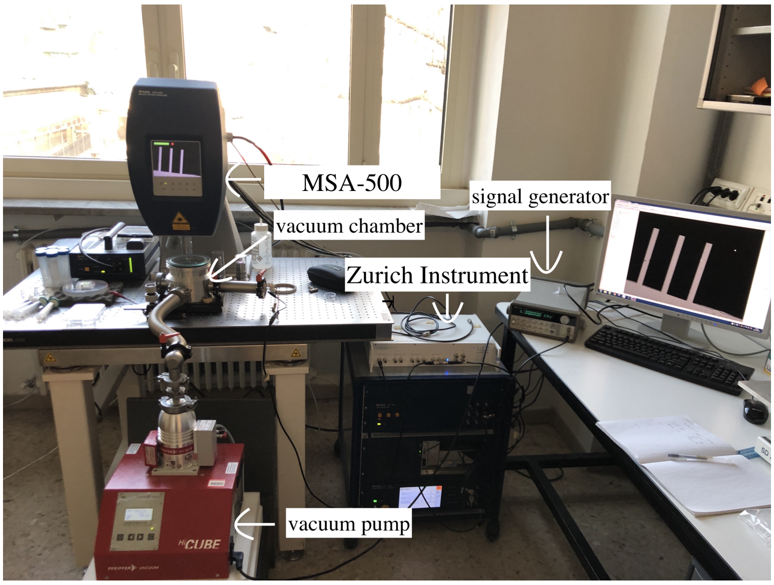

Figure 3.3: Experimental set up of our measure

And there is a vacuum pump connecting to the MSA-500 system, which is called Hicube. This machine provide a vacuum chamber in the MSA-500 system, in which micro and nano cantilevers are oscillating. To implement our measurement, a signal generator is used to export the excitation signal while the Zurich instrument exporting a continuum voltage. Combination of the signals is used to excite the piezoelectric element in the vacuum chamber in the MSA-500 system to realize Fano resonance in the micro and nano cantilever array MC24. A laser focuses on the tip of the microcantilever, the reflections of the laser from the vibrating microcantilever are read into to a PSD, converting vibrations into changing voltages. These voltages are sent to a lock-in amplifier that can extract a signal with a known carrier wave from an extremely noisy environment. In our measurement, the Zurich Instrument(HF2Li) is the lock-in amplifier that can transfer the signal into amplitudes and phases.A program is performed in Labview control the signal generator and the Zurich Instrument. These saved measure data are analyzed in an another commercial software which is called

Origin 2018.

3.3 Labview Software

To implement the observation shifts of Fano, the Labview program should control parameters of signal generator and Zurich Instrument HF2Li. Furthermore, the signal generator outputs a group of discrete excitation signals, uprising with a resolution one by one. During outputting the discrete excitation signal, the Zurich Instrument should sweep a appropriate window of frequency to record the position on which the laser is focused. Until the sweep measurement file is safely saved automatically, the program of Labview starts a new excitation voltage from the signal generator.

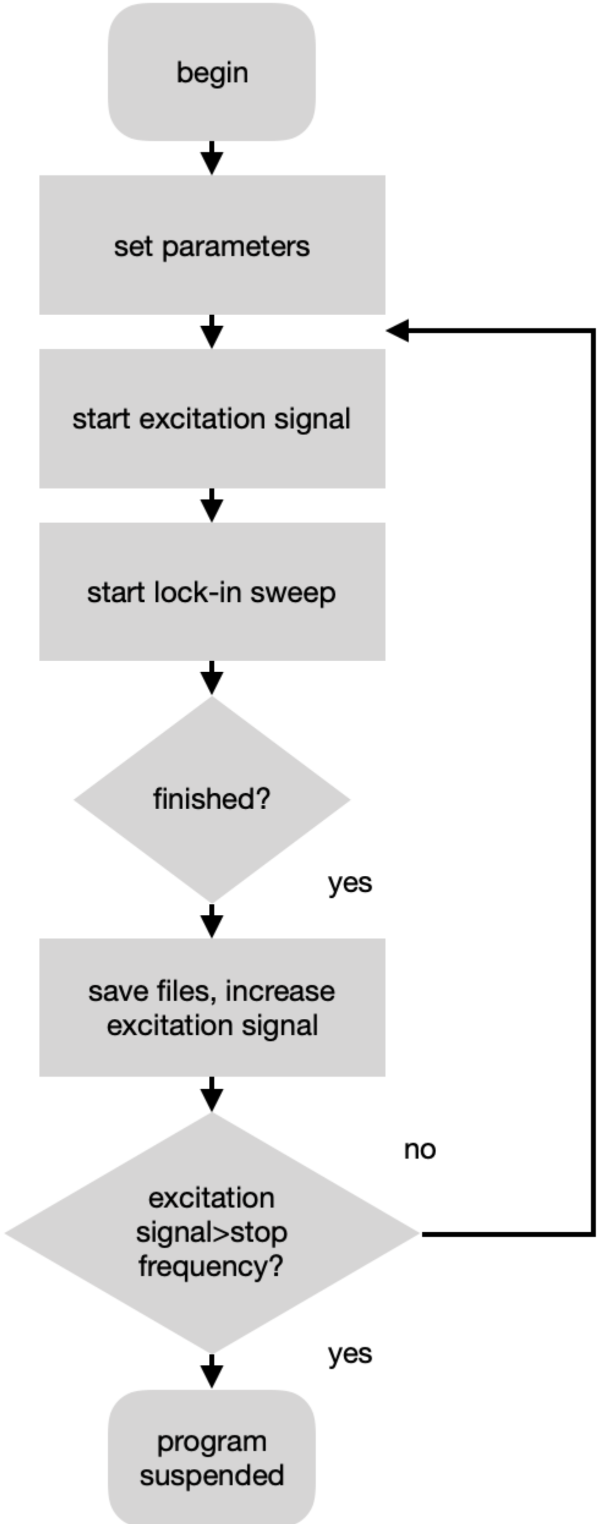

“

Figure 3.4: Flow chart of the Labview program

Thanks to the support driver from the signal generator and the user interface of Zurich Instrument itself is graphical. Both devices provide an example which are supportive in Labview. However, it is not a pure programming task. Inter kennels of the examples are protected. No edit can be performed into the example. Even algorithm is perfect, the two devices don't work as the program commands. Thanks to Zurich Instrument exporting a "finished" signal after the sweep finishes. This "finished" signal and "value(signaling)" of property node from Labview are used to start saving measurement files and a new excitation voltage from signal generator. By suitably activating and blocking property node and the "finished" signal in a while loop with the signal generator. The program is ready to measure.

Chapter 4

Measures and Results

4.1 Description of Measure

To better exploit the Fano resonance in micro and nano cantilever arrays, this measure is done by first picking a appropriate cantilever and exciting this cantilever by a group of discrete driven signal with a small resolution stepwise growing from a frequency below the resonance to one above. For every that discrete driven signal, the Zurich Instrument is used to record the Fano resonance from the cantilever weakly coupled to the first cantilever. After recording every Fano resonances by each driven signal. A commercial data analysis software(Origin 2018) is used to analyze the differences among every Fano resonances. In Figure 4.1, to begin our measure, a laser is focusing on the tip of a cantilever showing on the right of the figure. While on the left, with an appropriate excitation signal to the piezoelectric element, the resonance frequency and the corresponding Fano resonances from other cantilevers are shown on the figure. Among those Fano resonances, I pick stable one with less interferences to do our measure on it.

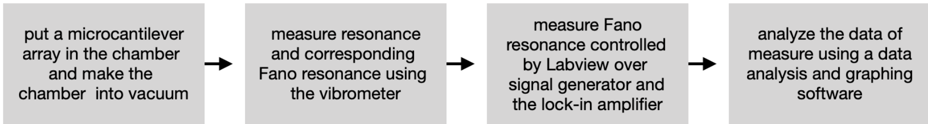

Figure 4.2: Steps of the measure method

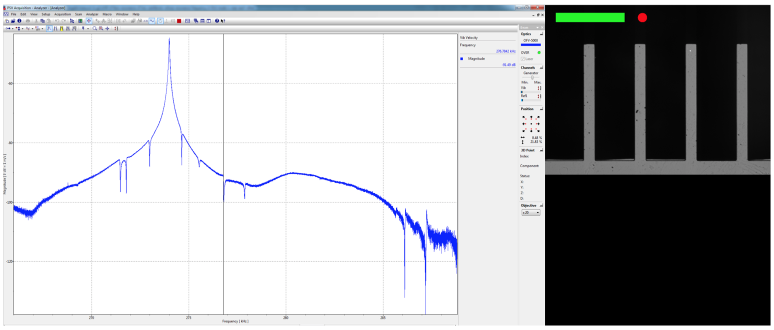

Figure 4.1: The vibrometer help us to find the resonance and the corresponding Fano resonances

A general method is described in Figure 4.2. After obtaining the resonance frequency and the corresponding Fano resonances, in our measure, we focus the laser on the tip of cantilever number 8 measuring Fano resonance coupled from number 9 while resonances in different mode of cantilever number 9 are excited.

And in returns, by the study of Fano resonance, the parameters affecting shifts of Fano resonances can be found. With these parameters, we can denote all other cantilevers' vibrating details by only measuring one cantilever and their corresponding Fano resonances. As previously discussed in Chapter one, Fano resonance can be different shapes with different parameter q. During the measure, many shapes were observed and used to explore features.

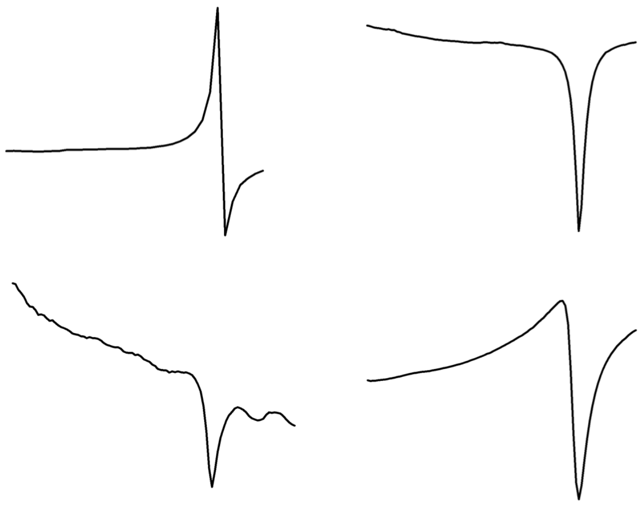

Figure 4.3: Different shapes of Fano resonance observed during measure

Coupling between modes happens due to the increased tension along the beam axis which changes the effective stiffness of the mechanical structure. [8] By the software I wrote, we can have more details of the results of changed effective stiffness of the mechanical structure. This figure explains what we are going to measure. First, we have a "sweep frequency window" indicating the frequency gap used by the Zurich Instrument to sweep. The "excitation signal" shows us the frequency of excitation voltages. This so-called waterfall figure can show us the shift of Fano resonance when excitation signals pass over the resonance frequencies of different modes. The micro cantilever we used is named as MC24-8-F9. 24 means the number of the micro cantilever. 8 is the number of the microcantilever(counting from the right to left) where the laser is focused on. F9 means the Fano resonance of number 9 microcantilever corresponding to number 8 microcantilever.

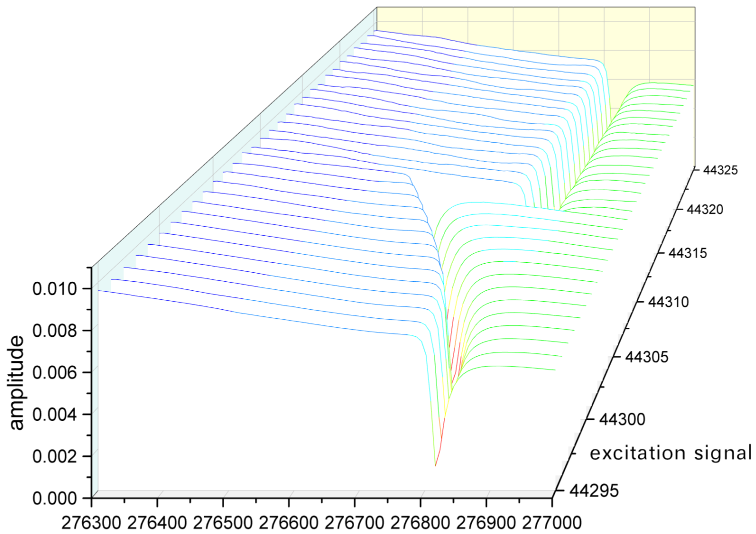

Figure 1: Waterfall method to show the result

Figure 4.4: A so-called waterfall method to show the measure

As in Figure 4.4, on the left, the excitation signals are indicated while on the bottom, the appropriate range to obtain the Fano resonance is shown, and on the right the amplitude of Fano resonances are shown. For each excitation signal, there is a recorded Fano resonance, we can see clearly that the Fano resonance shifts to the left which means the Fano resonance frequency decreases. In the following Figure 4.5, the contour of the shifting Fano resonance peaks are plotted in order to see how much the shift is.

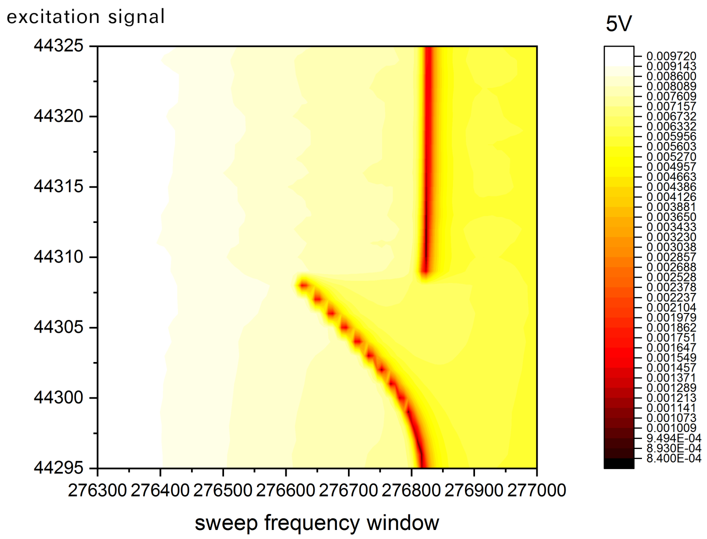

Figure 4.5: Another method(contour color fill) to show the measure

4.2 Results

These results are organized by indicating parameters affecting shifts of Fano resonance.

Compare different voltages

Measure in second mode while excitation signal in first mode

Here we present Fano resonances in second mode while excitation signal in first mode. Fano resonances are easy to observe in secone mode because more energy will excite the microcantilever array when excited in first mode. As we can observe in these figures, we can denote that the shifts become bigger along with the increasing excitation voltages. Shifts of Fano resonances vary with different measuring cantilevers. By comparing all the measures, we found the shifts of the Fano resonance are always to the left. In another word, the frequency of

Fano resonance decrease as the excitation signal increases. In the meanwhile, the amplitude of the Fano resonance remains the same. In the following Figure 4.6, from the contours lay on the left of the figure, we can denote that the bigger of the excitation signal, the more that the Fano resonance shifts to the lower frequency. The line on the right of each contour also shows the same behavior.

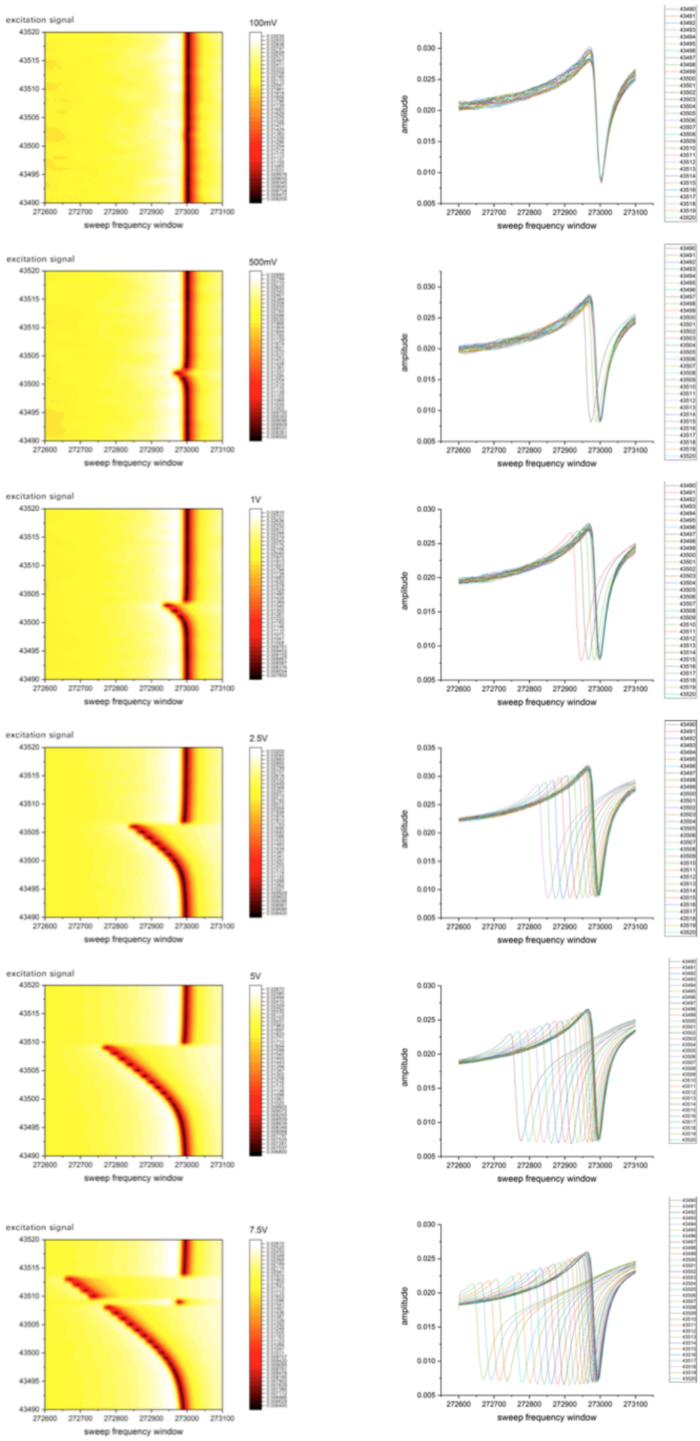

Figure 4.6: MC24-8-F5: measure results shown by contour of the peaks of the Fano resonance and shifts of the curve of the Fano resonance

Then I did the same measure from other Fano resonances corresponding to cantilever number 8 following the same method. Even other Fano resonances corresponding to other cantilevers show the same behavior.

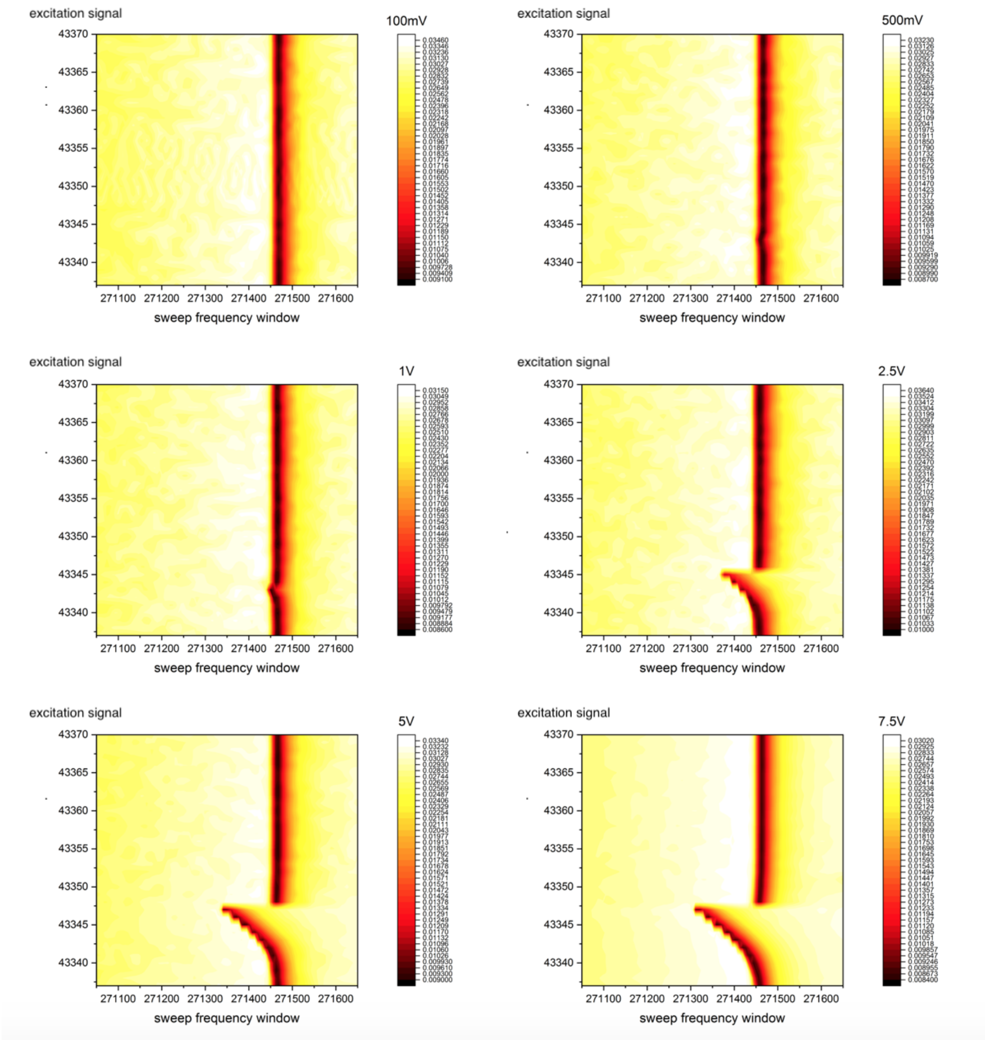

Figure 4.7: MC24-8-F7: different shifts of Fano resonance from microcantilever number 7 on number 8 as the excitation signal increases

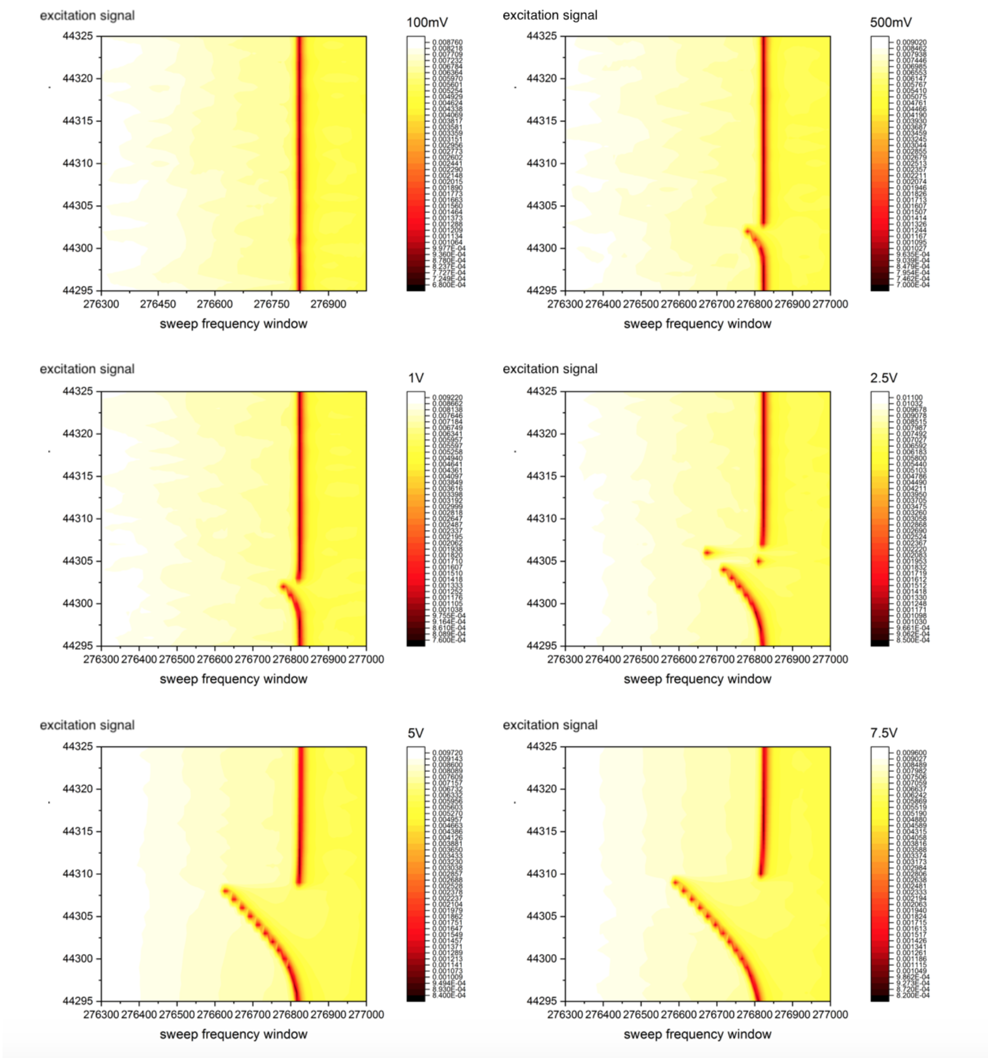

Figure 4.8: MC24-8-F9: different shifts of Fano resonance from microcantilever number 9 on number 8 as the excitation signal increases

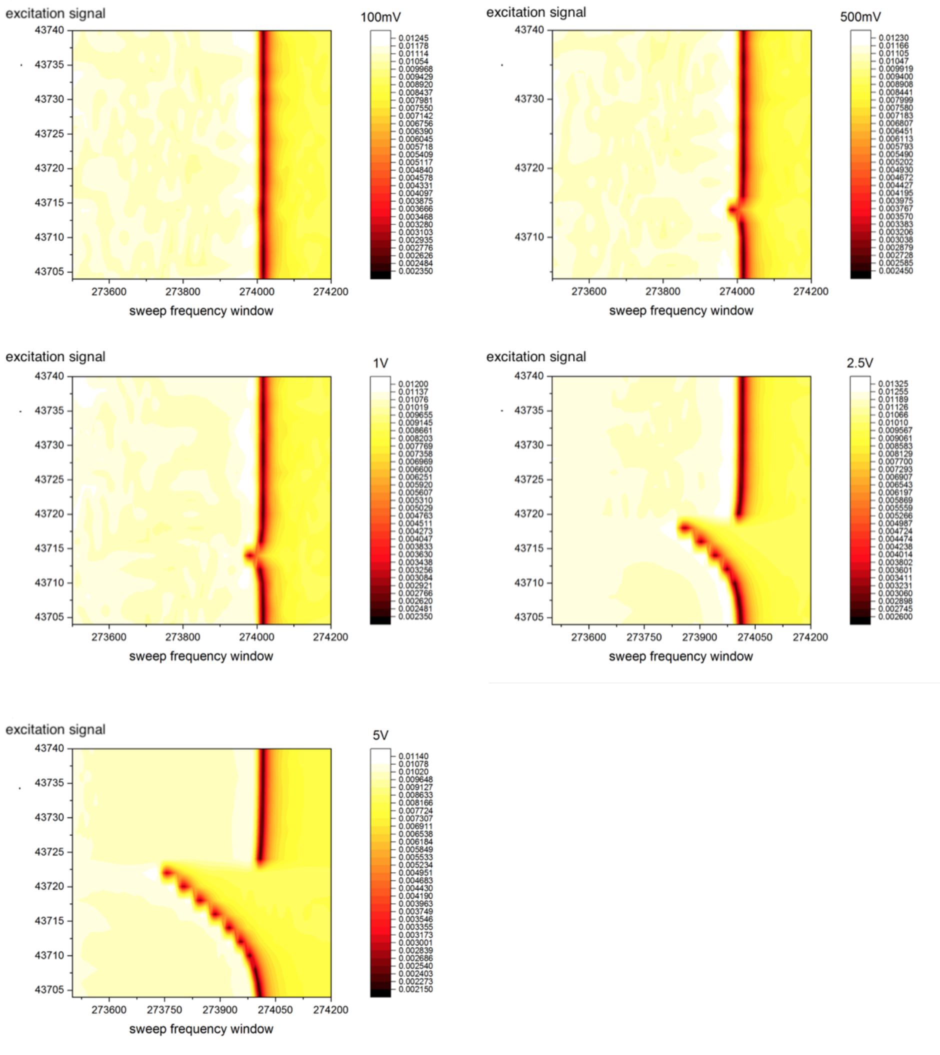

Figure 4.9: MC24-9-F8: different shifts of Fano resonance from microcantilever number 8 on number 9 as the excitation signal increases

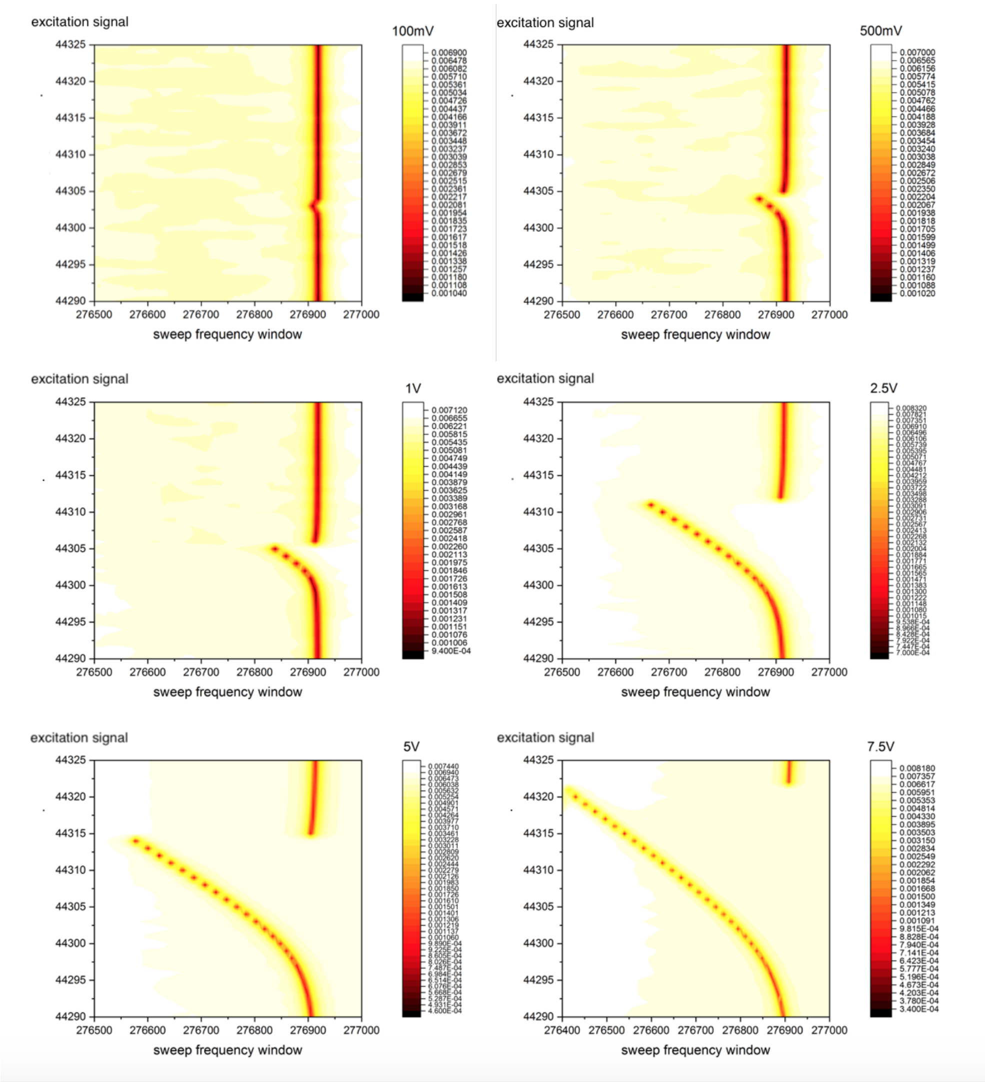

Figure 4.10: MC24-10-F9: different shifts of Fano resonance from microcantilever number 9 on number 10 as the excitation signal increases

Measure in third mode while excitation signal in first mode

To exploit more characteristics of Fano resonance in intermodal coupling. We started a new measure of Fano resonance in the third mode while the excitation signals are around the first mode.

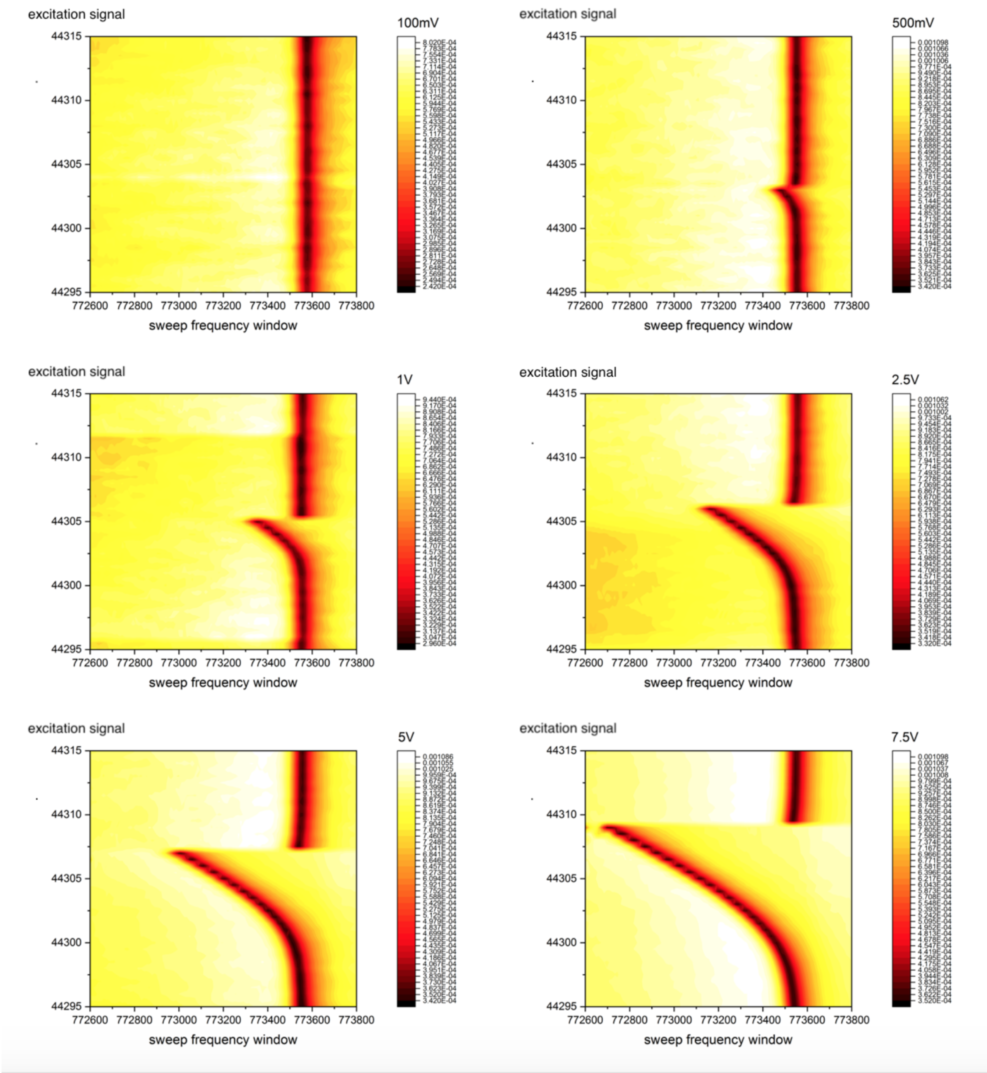

Figure 4.11: MC24-8-F9: different shifts of Fano resonance from microcantilever number 9 on number 8 as the excitation signal increases

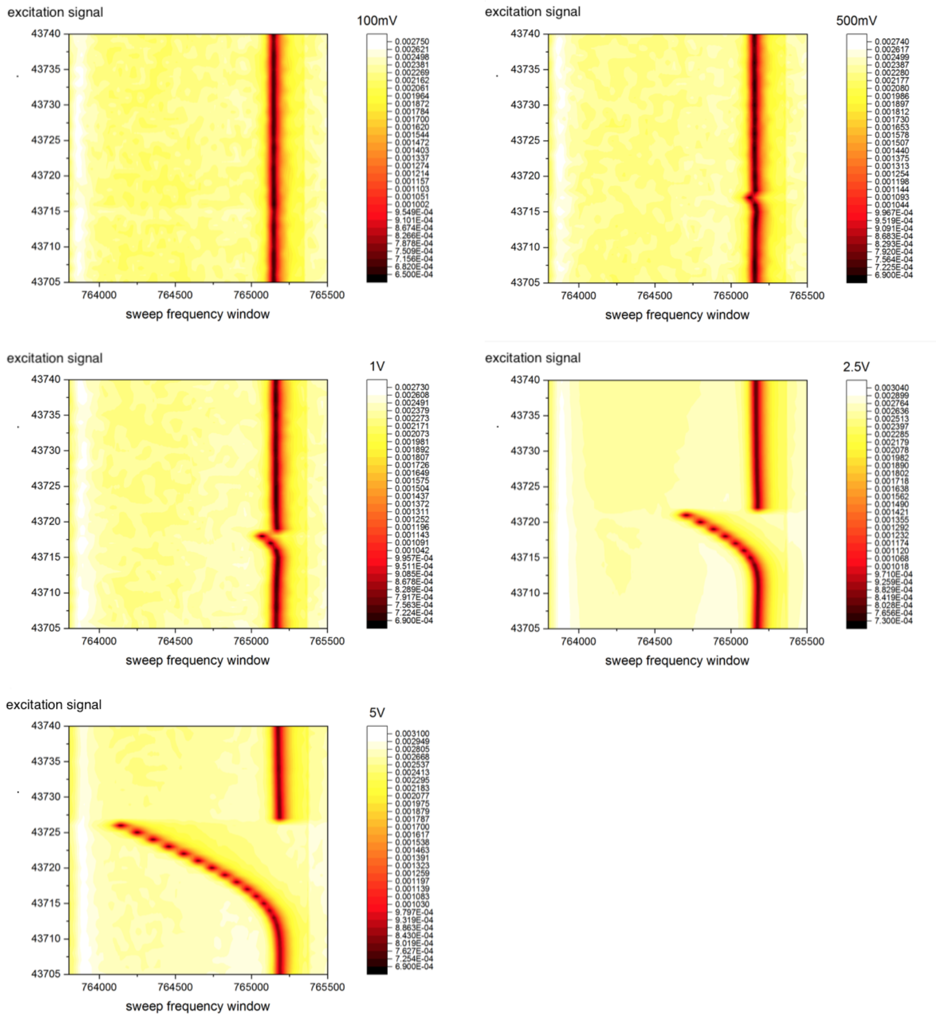

Figure 4.12: MC24-9-F8: different shifts of Fano resonance from microcantilever number 8 on number 9 as the excitation signal increases

By the results in Figure 4.11 and 4.12, we can denote that the Fano resonance in the third mode has the same behavior with the Fano resonance in the second mode, that is they shift to the lower frequency when the excitation signal becomes bigger. However the shifts of Fano resonance in the third mode are much bigger than the shifts in the second mode.

Measure first mode while excitation signal in second mode

Then we do the measure in an opposite way. The Fano resonance in the first mode is measured when excited in the second mode. This time the Fano resonance still shifts to the lower frequency when the excitation signal becomes bigger, but in the quite different way. That came to us with an idea that excitation signals in different modes can stiffen or soften the effective structure which can be induced by tension or displacement. This different shifting way of Fano resonance also brought us the measure of Fano resonance with decreasing excitation signals and increasing excitation signals in order to compare to the Duffing phenomenon in the next section.

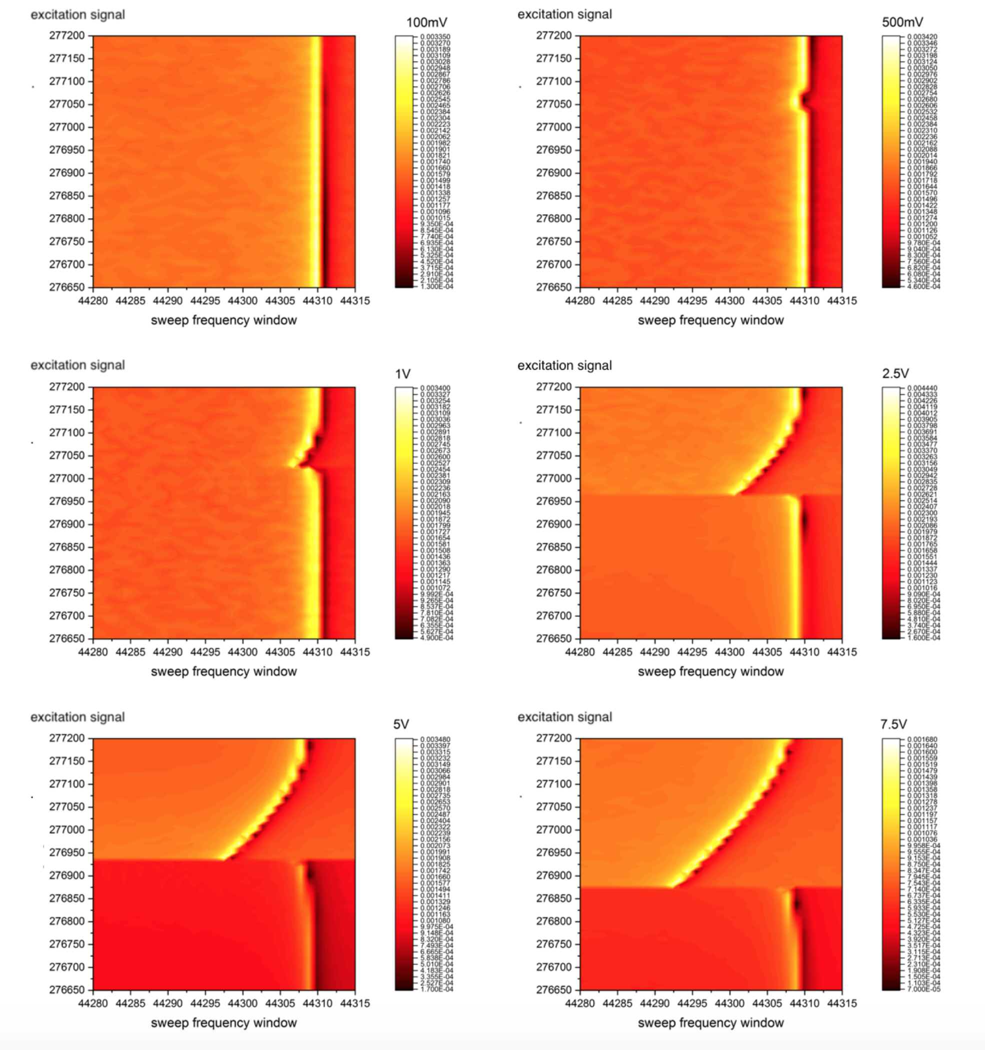

Figure 4.13: MC24-8-F9: different shifts of Fano resonance from microcantilever number 9 on number 8 as the excitation signal increases

By comparing different voltages, we can denote that shifts of Fano resonance is relative to excitation voltages and effective structure of a microcantilever causing displacement-induced tension. Since the maximum voltage the signal generator can export is 10V, we cannot find any shift in third mode while excitation signal in second mode, in second mode while excitation signals in third mode, in first mode while excitation signals in third mode.

Compare different modes while excitation signal in the same mode

In this subsection, we compare the results of measuring shifts of Fano resonance in second mode and in the third mode while the excitation signals are in the same first mode. We wanted to know exactly how much the shifts are between different modes.

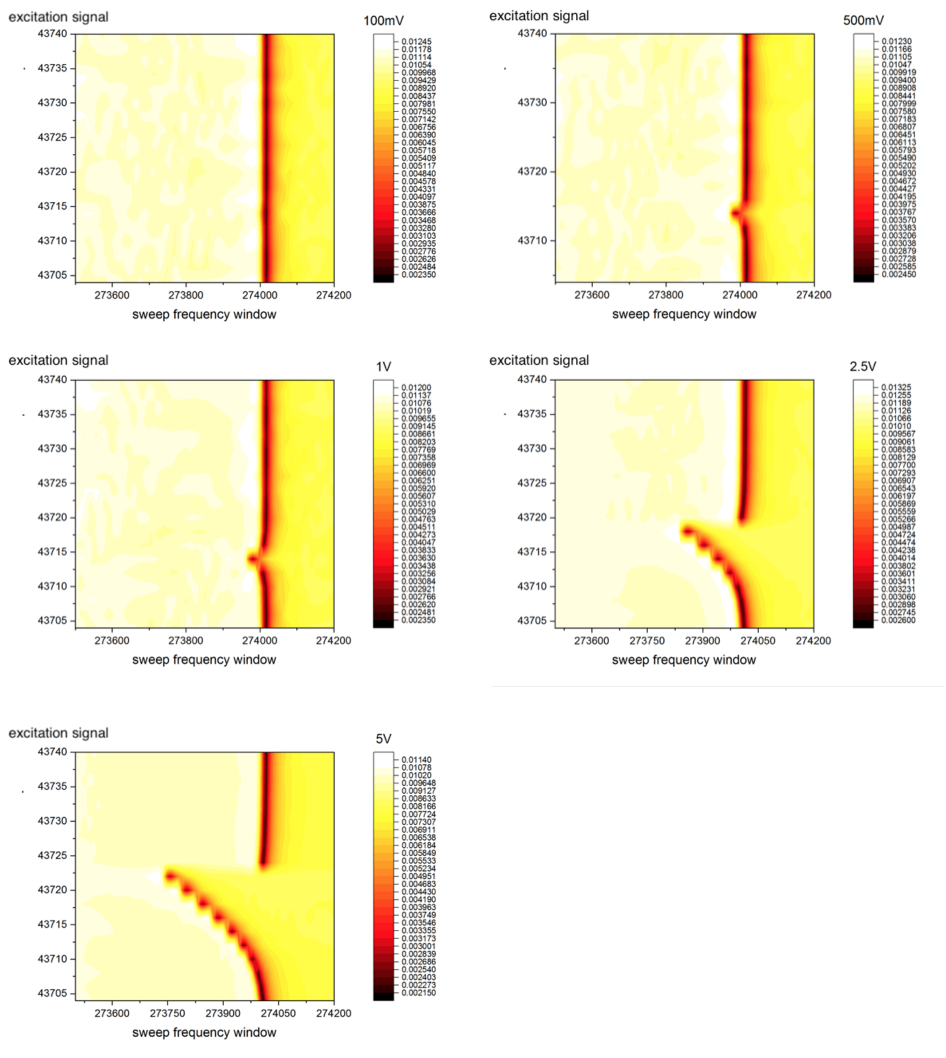

Figure 4.14: MC24-9-F8: different shifts of Fano resonance from microcantilever number 8 on number 9 as the excitation signal increases in second mode

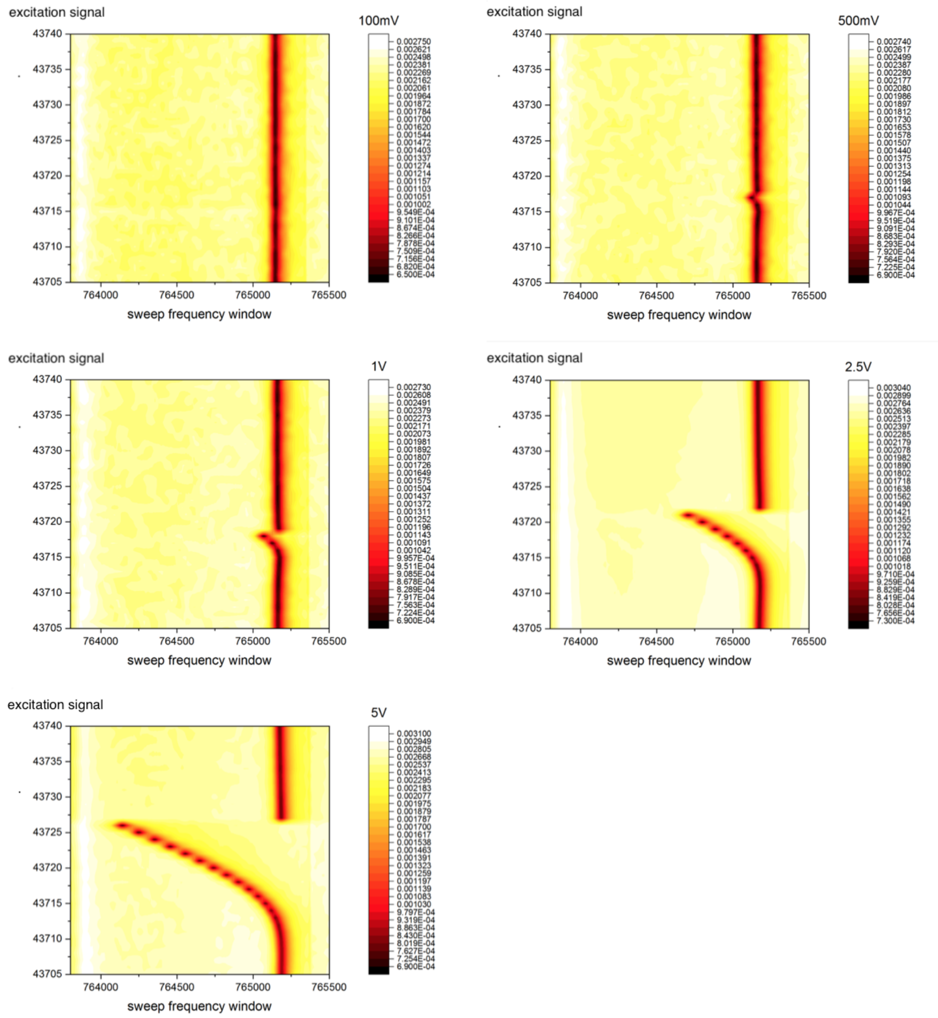

Figure 4.15: MC24-9-F8: different shifts of Fano resonance from microcantilever number 8 on number 9 as the excitation signal increases in third mode

Fano resonance from another measure

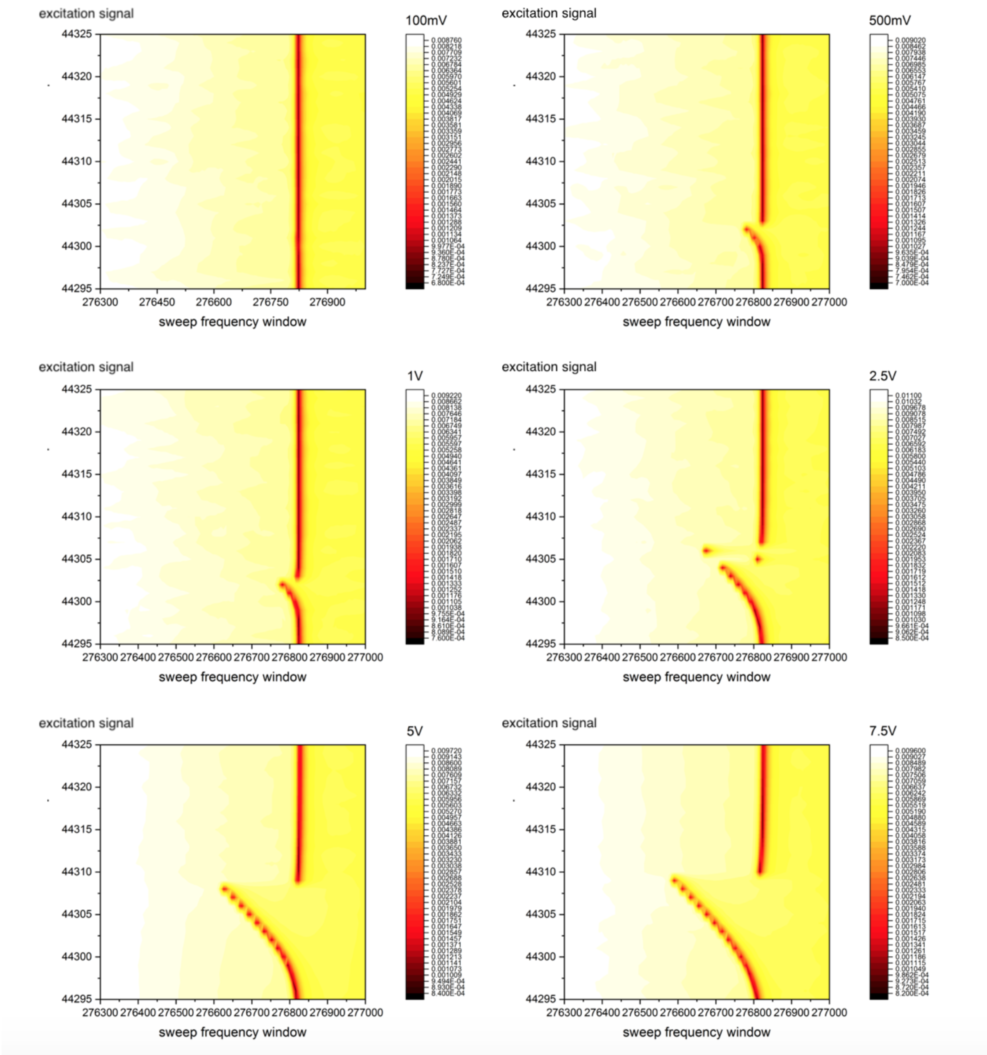

Figure 4.16: MC24-8-F9: different shifts of Fano resonance from microcantilever number 9 on number 8 as the excitation signal increases in second mode

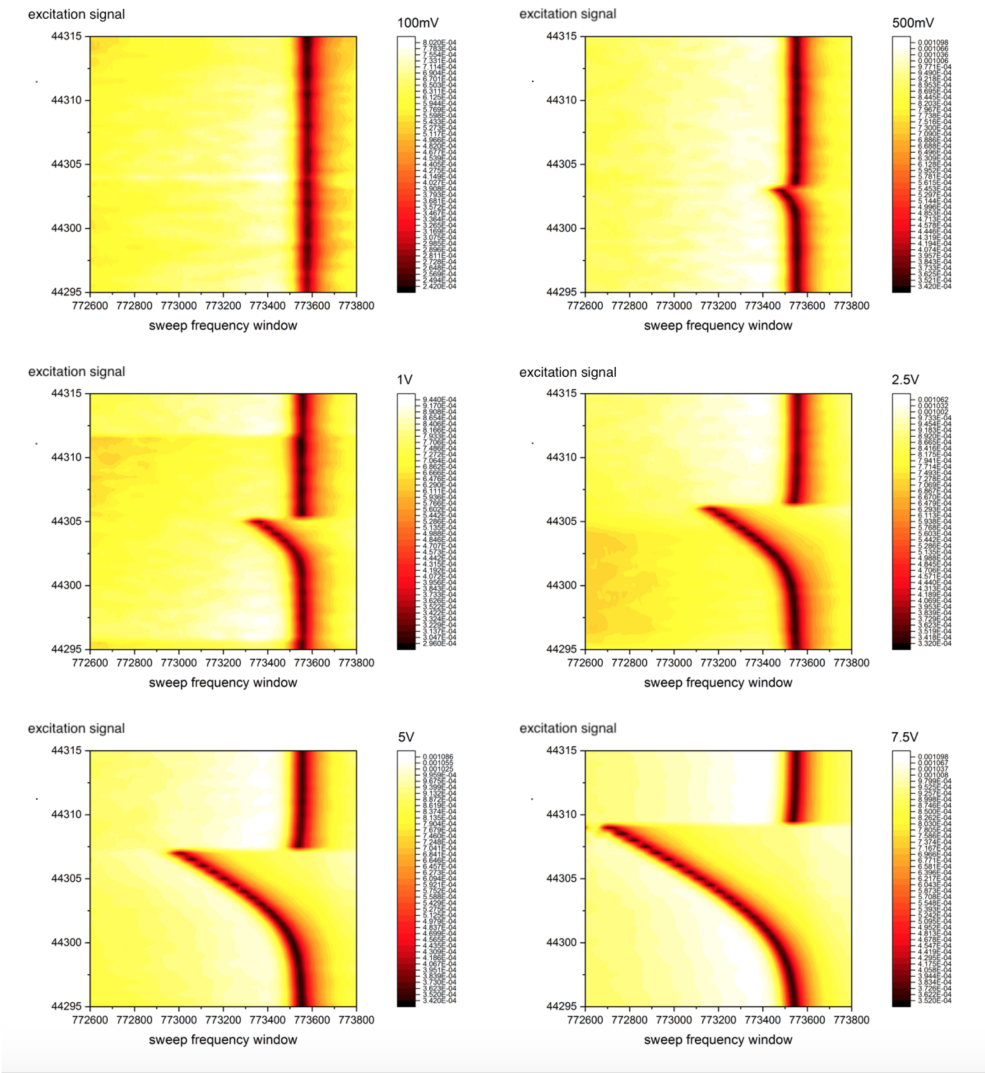

Figure 4.17: MC24-8-F9: different shifts of Fano resonance from microcantilever number 9 on number 8 as the excitation signal increases in third mode

From the Figure 4.14 and 4.15, 4.16 and 4.17, we can see that the shift of Fano resonance in third mode is bigger than that in second mode with the same excitation signals. In another word, shifts of Fano resonance in microcantilever arrays are relative to mode numbers.

excitation signal	Fano resonance 1-2	Fano resonance 2-1	Fano resonance 3-1
100mV	0	0	0
500mV	0.0023%	0.0046%	0.0016%
1V	0.0068%	0.0155%	0.0353%
2.5V	0.0226%	0.0538%	0.0552%
5V	0.0293%	0.0715%	0.0741%
7.5V	0.0406%	0.0845%	0.1132%

Table 4.1: Shifts of the Fano resonance are shown by $f_{shift}/f_{Fano\ resonance}$. 1-2 means: the Fano resonance is measured in the first mode while excitation signals are around the second mode

It is clear to see in the Table 4.1 that the shifts of Fano resonance become bigger when measured in higher mode.

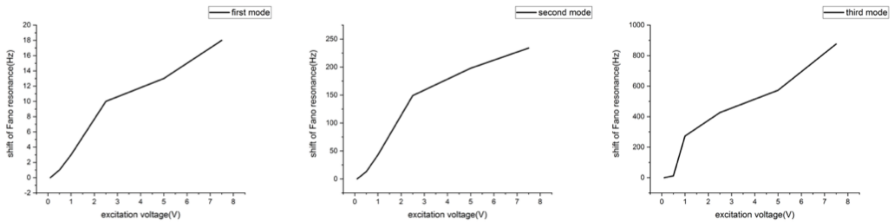

Figure 4.18: Plot of the data in Table 4.1 showing shifts of Fano resonance corresponding to excitation voltages. Fano resonance in first mode is on the left, in second mode is in the middle and in third mode is on the right

Based Figure 4.18 , we can't find a pattern whether the curve is linear or parabolic.

4.3 Compare with Duffing phenomenon

As mentioned in the theory chapter, the shape of the resonance frequency will tilt to right or left when increasing the excitation voltage. In second mode and third mode, we observed the Duffing phenomenon. Since the curve of the tilted shape is not symmetric, it will show different shapes when sweep from right to left and the opposite because of the "jump" which is mentioned in theory chapter. So we measured an appropriate Fano resonance with decreasing excitation signals and increasing excitation signals in order to see if there is a difference between two excitation method.

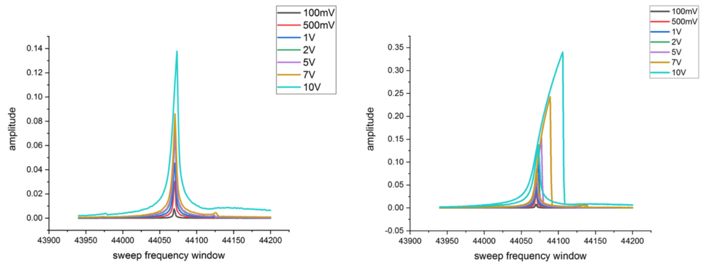

Figure 4.19: Duffing phenomenon of the resonance peak in first mode. The left figure shows the sweep of the resonance is from left to right while the right figure shows the result of bidirectional sweep

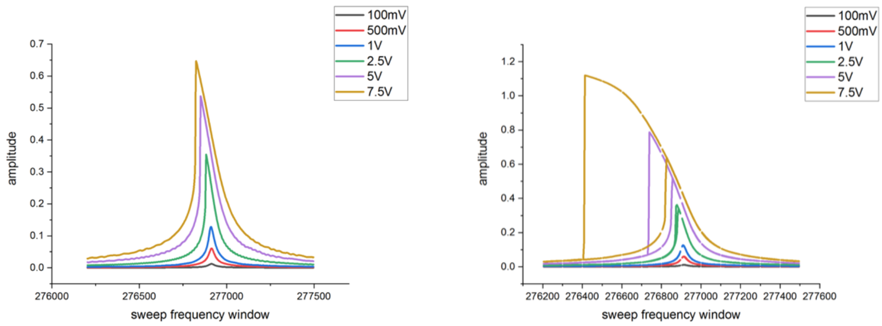

Figure 4.20: Duffing phenomenon of the resonance peak in second mode. The left figure shows the sweep of the resonance is from left to right while the right figure shows the result of bidirectional sweep

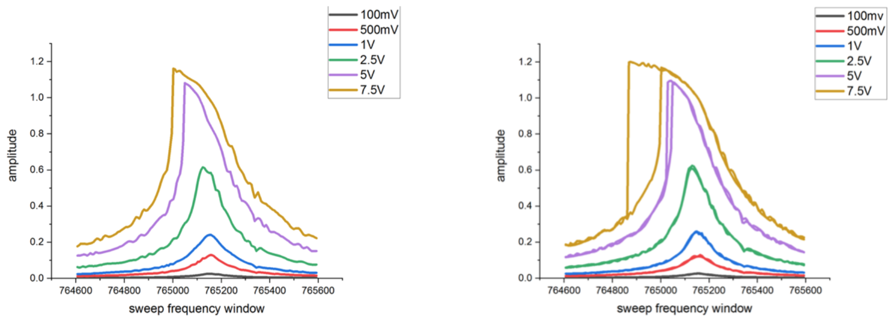

Figure 4.21: Duffing phenomenon of the resonance peak in third mode. The left figure shows the sweep of the resonance is from left to right while the right figure shows the result of bidirectional sweep

As for shifts of Fano resonance, direct observations can provide the evidence that shifts of Fano resonance have the similar phenomenon with the Duffing phenomenon. For Fano resonance on one particular microcantilever, the excitation signal exports in increasing and decreasing way. The shifts of both Fano resonances should be different. And the results are shown in Figure 4.19, 4.20 and 4.21. In second mode and third mode, the increasing excitation signals soften the effective structure which can be induced by tension or displacement in the microcantilever array.

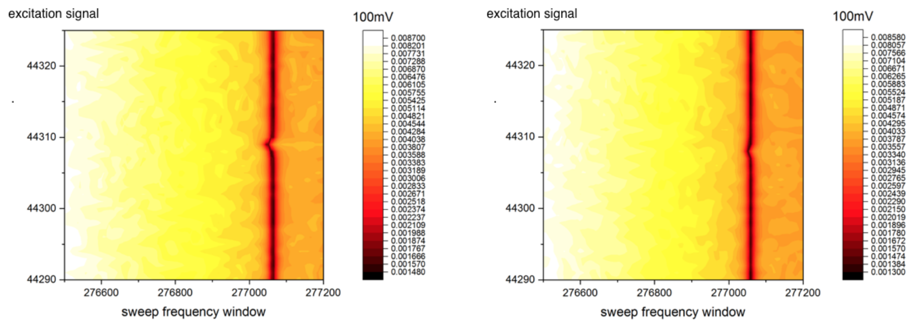

Figure 4.22: Shift of Fano resonance with decreasing excitation signals(100mV) on the left while increasing ones on the right

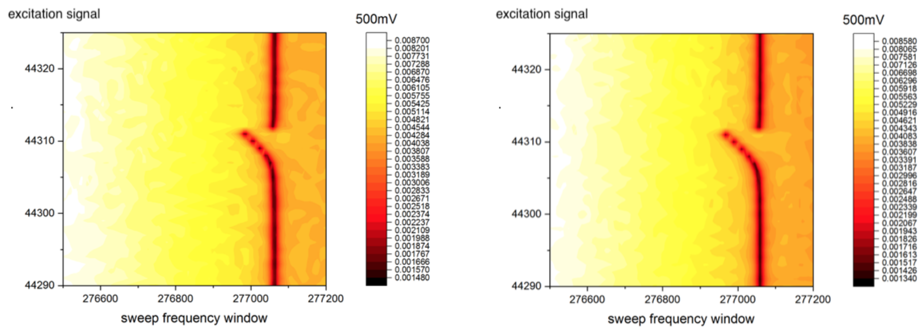

Figure 4.23: Shift of Fano resonance with decreasing excitation signals(500mV) on the left while increasing ones on the right

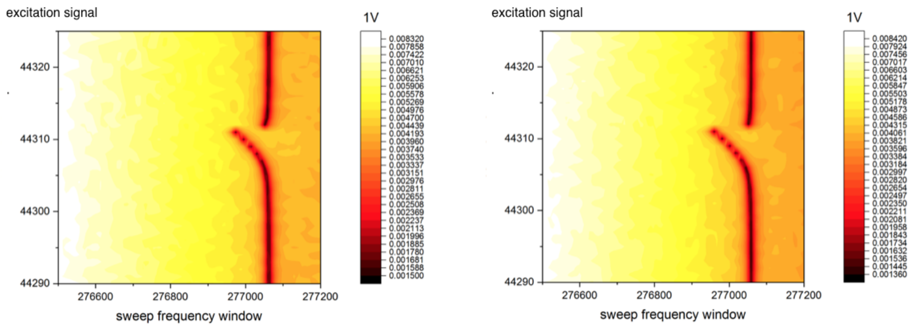

Figure 4.24: Shift of Fano resonance with decreasing excitation signals(1V) on the left while increasing ones on the right

For the excitation signal below 1V, there is no obviously difference between decreasing excitation signals and the increasing ones. But for the excitation signal above 2.5V, the difference of the shifts between decreasing signals and increasing signals is quite obvious.

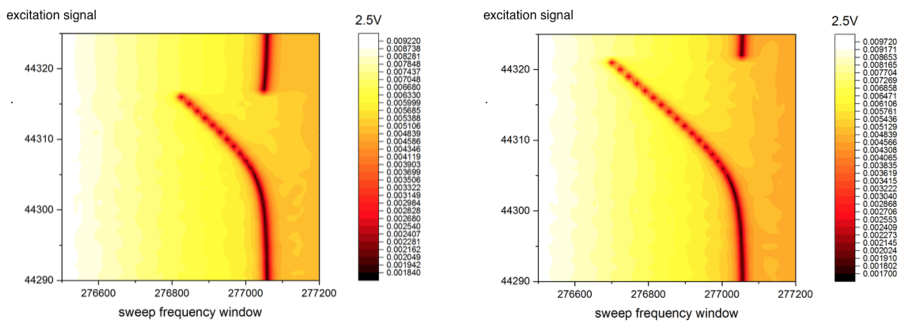

Figure 4.25: Shift of Fano resonance with decreasing excitation signals(2.5V) on the left while increasing ones on the right

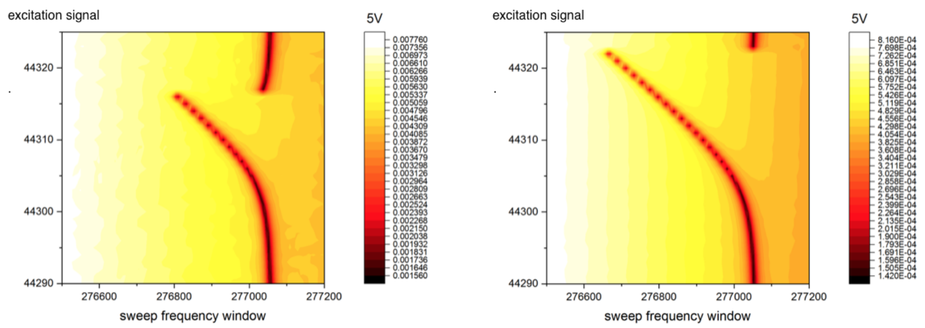

Figure 4.26: Shift of Fano resonance with decreasing excitation signals(5V) on the left while increasing ones on the right

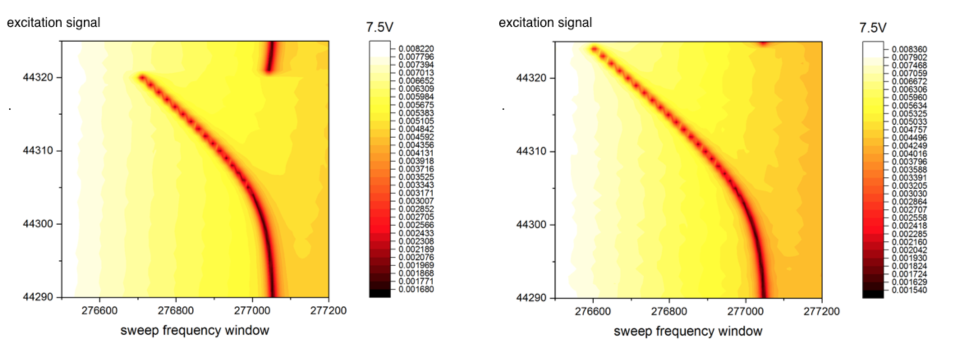

Figure 4.27: Shift of Fano resonance with decreasing excitation signals(7.5V) on the left while increasing ones on the right

By plotting different shifts of Fano resonance excited by decreasing signals in one graph, we can see clearly that the same Duffing phenomenon exists in Fano resonance with in normal resonance.

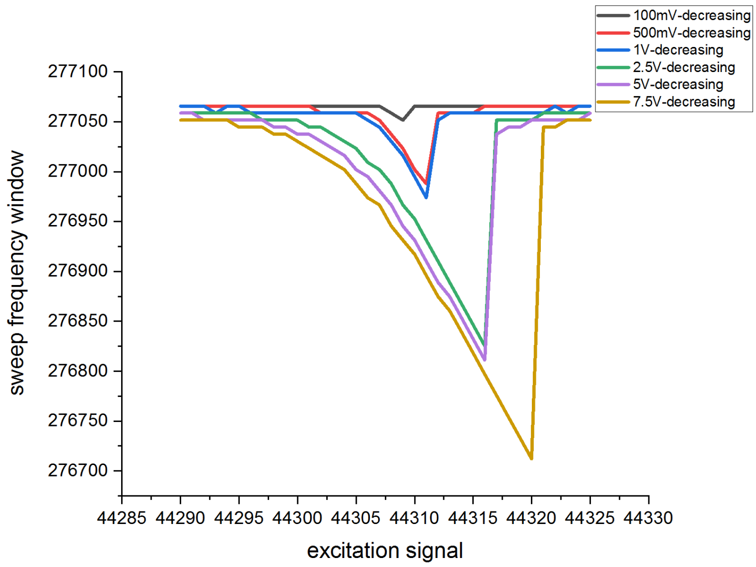

Figure 4.28: Shifts of Fano resonance excited by decreasing signals

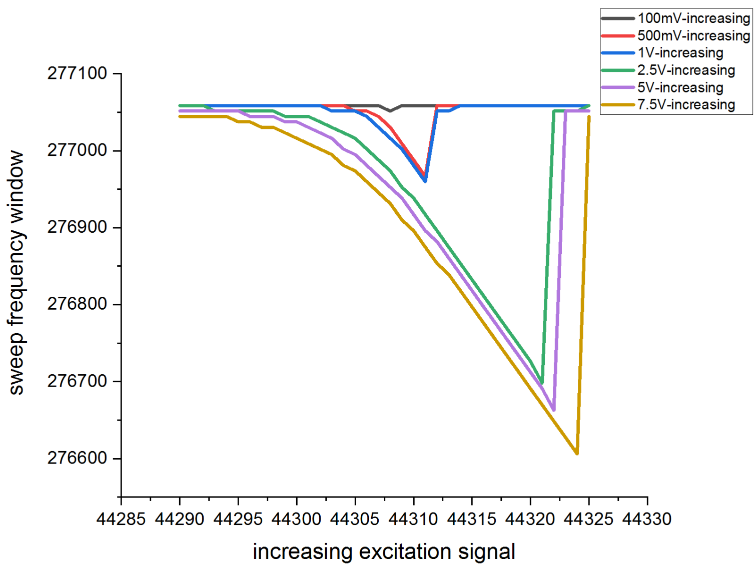

Figure 4.29: Shifts of Fano resonance excited by increasing signals

And we plot both shifts of Fano resonance excited by decreasing signals and increasing signals with the same excitation voltage. Then we can see the "jumps" phenomenon that happens in Fano resonance.

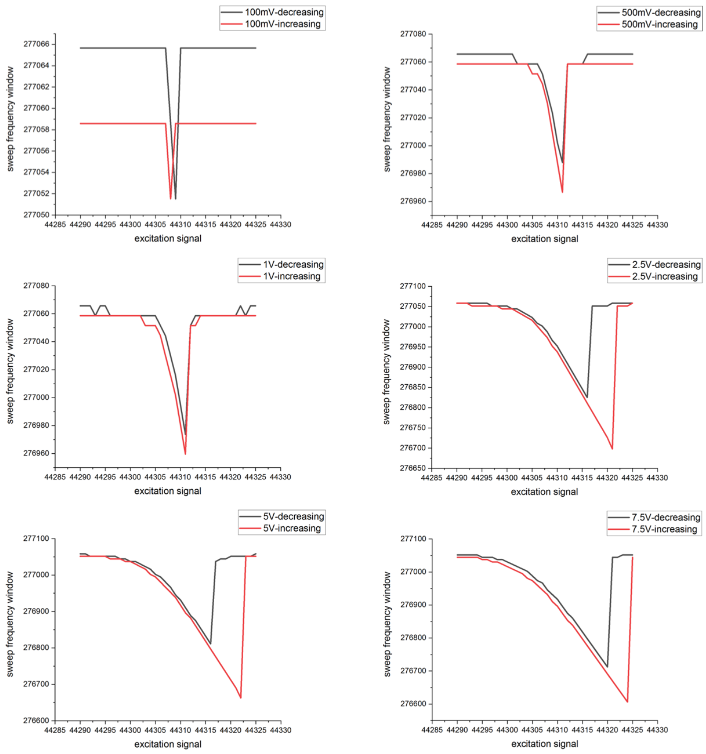

Figure 4.30: Comparison between shifts of Fano resonance excited by decreasing signals and increasing signals with the same excitation voltage

excitation signal	decreasing excitation signals	increasing excitation signals
100mV	0.0036%	0.0036%
500mV	0.0289%	0.0339%
1V	0.0314%	0.0364%
2.5V	0.0848%	0.1310%
5V	0.0899%	0.1436%
7.5V	0.1256%	0.1639%

Table 4.2: Shifts of the Fano resonance are shown by $f_{shift}/f_{Fano\ resonance}$ in the table. There is a quite difference between decreasing excitation signals and increasing excitation signals

These clear evidences in Table 4.2 can help us to denote the numerical description of the shift by studying the Duffing phenomenon.

Chapter 5

Conclusions and Future works

5.1 Conclusions

In our measure, the Fano resonance is used as a tool to study the intermodal coupling among cantilevers in a microcantilever array. The excitation signal can stiffen or soften the effective structure of the microcantilever array which can be induced by tension or displacement. That depends on which mode the excitation signal is in. For our study, if the excitation signal is in second and third mode, it softens the effective structure while the excitations signal is in first mode, it stiffens the effective structure.

For weakly non linear coupled cantilevers in a microcantilever array, the Fano resonance peak can be used as a new peak with respect to the Lorentzian peak to detect mass. Using Fano resonance can greatly decrease the measuring time by paralleling measurement and the detectable mass. To implement that, detailed behaviors of Fano resonances in non linear coupled cantilevers is studied. As the excitation signal increases, the Fano resonance shifts to a lower frequency. And those shift behaviors are different between decreasing excitation signals and increasing excitation signals the same with the Duffing phenomenon.

5.2 Future works

There is a lot to do in the future. More and more measures should be done to numerically draw an equation to describe the behavior of shift of Fano resonance in weakly coupled cantilevers of a microcantilever array.

And during the measure, there is an interesting discovery. The Fano resonances of number 9 and 11 corresponding to number 8 are near each other while their resonance frequencies in the first mode are also enough near each other. So when the excitation signal is in the first mode, the Fano resonance of number 11 shifts to the location of Fano resonance of number 9, and the two Fano resonances merge together. That is interesting because that phenomenon shows us the Fano resonances are not independent among each others. They can easily merge and separate just like transferring waves in Figure 5.1.

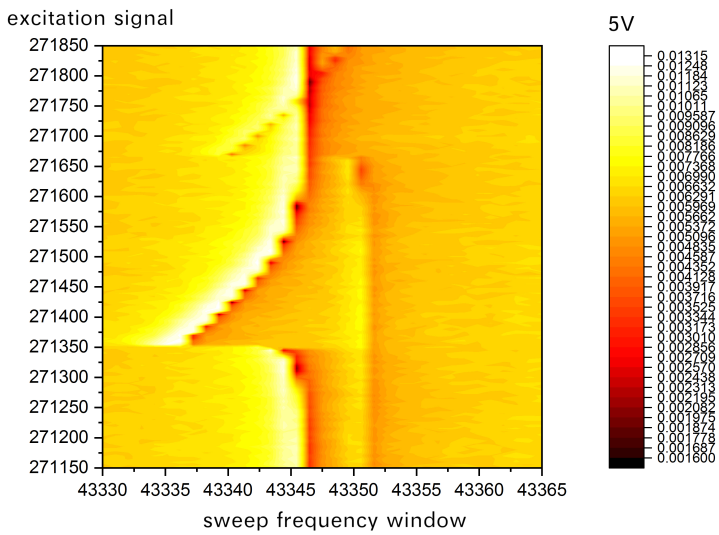

Figure 5.1: Fano resonance on the right shifts to the location of Fano resonance on the left

It is better to see the procedures of the merge in amplitude and phase in Figure 5.2 and 5.3.

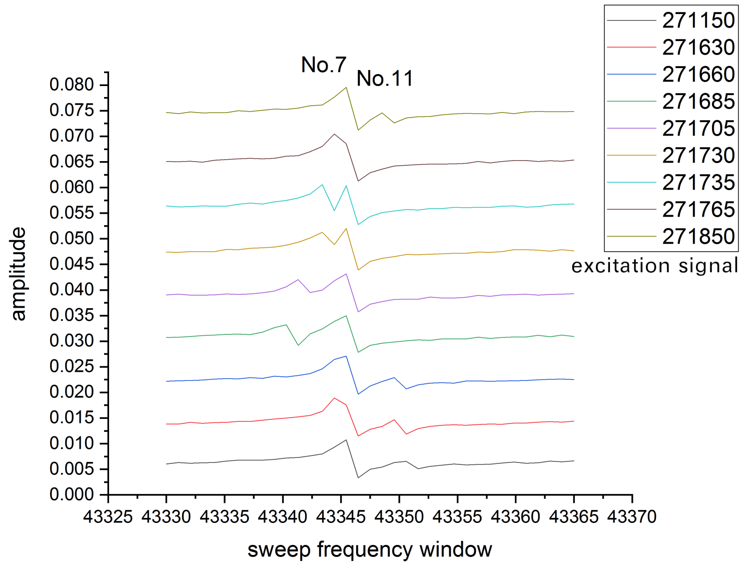

Figure 5.2: Merge of Fano resonances in amplitude

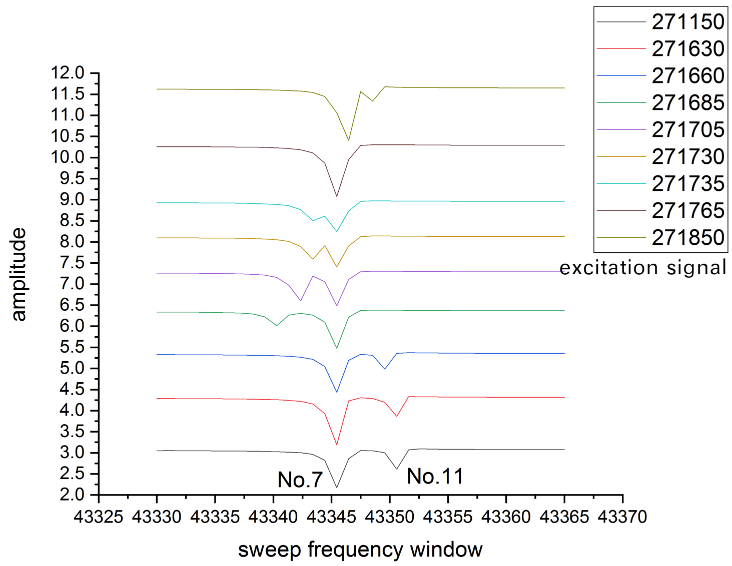

Figure 5.3: Merge of Fano resonances in phase

This is also worthy to study in the future to better understand the behavior of Fano resonance in weakly coupled cantilevers in a microcantilever array.

References

[1] C. Ricciardi, G. Canavese, R. Castagna, I. Ferrante, A. Ricci, S. L. Marasso, L. Napione, and F. Bussolino, "Integration of microfluidic and cantilever technology for biosensing application in liquid environment," *Biosensors and Bioelectronics*, vol. 26, no. 4, pp. 1565–1570, 2010. vi, 4, 5

[2] A. E. Miroshnichenko, S. Flach, and Y. S. Kivshar, "Fano resonances in nanoscale structures," *Reviews of Modern Physics*, vol. 82, no. 3, p. 2257, 2010. vi, 6

[3] S. Stassi, A. Chiadò, G. Calafiore, G. Palmara, S. Cabrini, and C. Ricciardi, "Experimental evidence of fano resonances in nanomechanical resonators," *Scientific reports*, vol. 7, no. 1, p. 1065, 2017. vi, 7, 8, 21

[4] S. Schmid, L. G. Villanueva, and M. L. Roukes, *Fundamentals of nanomechanical resonators*, vol. 49. Springer, 2016. vi, 9, 12, 13, 17, 19

[5] M. Brennan, I. Kovacic, A. Carrella, and T. Waters, "On the jump-up and jump-down frequencies of the duffing oscillator," *Journal of Sound and Vibration*, vol. 318, no. 4-5, pp. 1250–1261, 2008. vi, 23

[6] D. Jordan and P. Smith, *Nonlinear ordinary differential equations: an introduction for scientists and engineers*, vol. 10. Oxford University Press on Demand, 2007. vii, 24

[7] M. Matheny, L. Villanueva, R. Karabalin, J. E. Sader, and M. Roukes, "Nonlinear mode-coupling in nanomechanical systems," *Nano letters*, vol. 13, no. 4, pp. 1622–1626, 2013. vii, 26

[8] A. B. Arı, M. Ç. Karakan, C. Yanık, İ. İ. Kaya, and M. S. Hanay, "Intermodal coupling as a probe for detecting nanomechanical modes," *Physical Review Applied*, vol. 9, no. 3, p. 034024, 2018. vii, 26, 27, 39

[9] K. Asadi, J. Yu, and H. Cho, "Nonlinear couplings and energy transfers in micro-and nano-mechanical resonators: intermodal coupling, internal resonance and synchronization," *Philosophical Transactions of the Royal Society A: Mathematical, Physical and Engineering Sciences*, vol. 376, no. 2127, p. 20170141, 2018.

[10] S. Zaitsev, O. Shtempluck, E. Buks, and O. Gottlieb, "Nonlinear damping in a micromechanical oscillator," *Nonlinear Dynamics*, vol. 67, no. 1, pp. 859–883, 2012.

[11] L. Villanueva, R. Karabalin, M. Matheny, D. Chi, J. Sader, and M. Roukes, "Nonlinearity in nanomechanical cantilevers," *Physical Review B*, vol. 87, no. 2, p. 024304, 2013.

[12] N. Kacem, S. Hentz, D. Pinto, B. Reig, and V. Nguyen, "Nonlinear dynamics of nanomechanical beam resonators: improving the performance of nems-based sensors," *Nanotechnology*, vol. 20, no. 27, p. 275501, 2009.

[13] T. J. Ryan, J. A. Judge, J. F. Vignola, and A. A. Glean, "Noise sensitivity of a mass detection method using vibration modes of coupled microcantilever arrays," *Applied Physics Letters*, vol. 101, no. 4, p. 043104, 2012.